第14回数理科学コンクール課題解説

平成23年11月3日 千葉大学先進科学センター

目 次

はじめに

明治の文明開化以来, 我が国は欧米先進国の科学技術を効率よく吸収して発展してきました. 戦後もこの傾向は基本的には変わっていません. 現在, 我が国は大量の自動車や電子機器を輸出して経済大国となっていますが, これらの工業製品の基本原理はほとんど外国で考えられたものです. 欧米諸国との間に経済摩擦や文化摩擦が生じている現状を考えると, これからの我が国で大切なことは独創性のある個性的な人材を育成して, 新しい科学技術のフロンティアを切り開き, 世界に貢献することであると考えられます.

千葉大学では, 日本のみならず, 世界の科学技術の先端を担う若者を発掘し, 育成するための一助として, 本年度も, 第 14 回数理科学コンクールを開催しました. このコンクールの特色は次の通りです.

1. 自由にゆったり考える

   試験時間は 6 時間, 途中の休憩や参考書・ノート等の持ち込みは自由とする.

2. たのしい物理・数学の発見

   物理や数学のカリキュラムにとらわれず, 物理や数学の本質に根ざした, 考えて楽しい問題を提供する.

3. 多彩な才能の評価

   様々な参加者の優秀な能力やユニークな発想を多面的に評価するため, 問題をたくさん解いたものだけでなく, 1 題に集中してすばらしい発想を出したものも表彰の対象にする. また, グループとしての総合能力を評価するため, 個人参加だけでなく, グループ参加も認める.

4. 人材の育成

   コンクール参加者の物理や数学の能力をさらに高めるため, コンクールの表彰式と講評会を行う.

過去 13 回のコンクールに引き続き, 多くの中高生の参加者があり, 楽しい雰囲気の中で, いろいろユニークなアイディアが生まれました. 中学生も, 高校生に負けず優秀でありました. そして, 答案を見ると, それぞれの問題に興味を持ちながら解答していることが読んでとれました.

第 14 回数理科学コンクールの課題の解説と提出された答案の評価を以下にまとめます. 解説に述べてあるように, 各課題は課題出題者の周りにある基本的な問題や最先端の問題, さらには歴史的に意味のある問題を元にして作成しました. 課題提出者一同, みなさんの素晴らしい洞察力と表現力を前にして, 大変感心いたしました.

参加者の皆さんが今後, 科学する心を磨き続け, 我国の科学の発展に貢献することを課題作成者一同希望します. 今後も諸君と共に科学することを楽しみたいと考えています. 千葉大学では今後も引き続きこのコンクールを実施する予定です. 物理・数学に興味がある中高生の積極的な参加を期待しています. 課題作成者もさらに研鑽をかさね, おもしろく, しかも科学の本質に迫る課題を考ていきます.

課題作成者

千葉大学教授　井宮　淳
東京慈恵会医科大学教授　植田　毅
(五十音順)

平成 23 年 11 月 3 日

優秀者氏名

平成23年7月17日に開催しました第14回数理科学コンクールの参加者の皆さんのすばらしい答案の中から以下の参加者諸君を表彰することを決定しました.

第14回数理科学コンクール優秀者

金欅賞	松谷優輝
	グループ1 保坂 駿 古坂拓朗 渡部和宏
	グループ24 後藤 倫 嶌田大吾 伊藤 駿
銀欅賞	小松玉麻果
	大舘賢人
	グループ11 萩原史織 藪﨑清圭 木村真由帆
	グループ18 笠井千晶 猪狩沙那
	グループ21 高橋健太
	グループ25 石橋和也 伊庭尚宏 花渕太一
	グループ27 谷井嶺太 鈴木陽太 綾部貴仁
学長賞	グループ20 菊池大海 稲嶺盛瑛 大熊浩章
	グループ28 梶原勇希 郡山巧人 木内 萌

課題	参加者名
1	松谷優輝
	大舘賢人
	グループ 1 保坂 駿 古坂拓朗 渡部和宏
	グループ 11 萩原史織 藪﨑清圭 木村真由帆
	グループ 18 笠井千晶 猪狩沙那
	グループ 24 後藤 倫 嶌田大吾 伊藤 駿
	グループ 25 石橋和也 伊庭尚宏 花渕太一
2	小松玉麻果
	グループ 1 保坂 駿 古坂拓朗 渡部和宏
	グループ 21 高橋健太
	グループ 24 後藤 倫 嶌田大吾 伊藤 駿
	グループ 27 谷井嶺太 鈴木陽太 綾部貴仁
	グループ 28 梶原勇希 郡山巧人 木内 萌
3	松谷優輝
	グループ 20 菊池大海 稲嶺盛瑛 大熊浩章
	グループ 24 後藤 倫 嶌田大吾 伊藤 駿
	グループ 28 梶原勇希 郡山巧人 木内 萌
4	グループ 1 保坂 駿 古坂拓朗 渡部和宏
	グループ 28 梶原勇希 郡山巧人 木内 萌

千葉大学先進科学センター長
教授 中山隆史

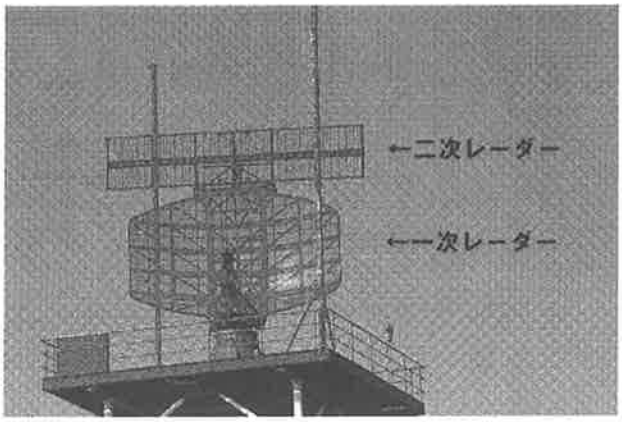

図 1: 金属の格子でできたレーダー

1　課題 1

課題

深さが一定の海岸があるとする. 海岸一帯に波が立たない水域を作りたい. 波面は直線的に進むがその速さは水深の平方根に比例します. 海底の構造を工夫してそれを実現するにはどのようにすればよいか考えてください. できるだけ労力を少なくするにはどうすればよいかを考えてください.

ただし, 波が崩れていない領域で海底に構造を作るものとします. また, 波の周波数（波長）は 1 種類として考えてください.

解説

この課題はもちろん東日本大震災で津波の圧倒的な破壊力で防潮堤が無残にも打ち砕かれたことを意識したものではありますが, もっと広く身近な現象と関連していることを意識して, 統一的な思考を身に着けてもらおうということで出題しました.

横波は弦の振動を考えればわかるように, 波を伝えるもの（媒体）が波の進行方向に位置を変えることなく進行方向に対して振動するものです. 水面の波では波の山近傍では水が回転運動をしていますが, 基本的には水の移動は伴いません. それに対し, 津波は海底の地形が変形することにより, 押し上げられたり, 落ち込んだりしたものを補填するために水の流れが発生するもので, いわゆる波とは全く振舞いが異なります.

さて, この課題では振動している波を考えてもらいました. 防潮堤などのような壁を作らなくとも波は遮ることができるということを考えてもらうのが目的でした.

この現象は身の回りで非常に多く利用されています. 例えば, 電子レンジの窓についている金属製の網, 図 1 に示すような金属の網のようなレーダーなど. これらは, 一定の間隔で周期的に金属の棒などを並べるとその間隔の 2 倍以上の波長（波の山と山の（もしくは, 谷と谷の）間の距離）の電磁波は反射されるという性質を用いています. 自然界でもこの現象を用いている例が沢山あります. 図 2 に示すモ

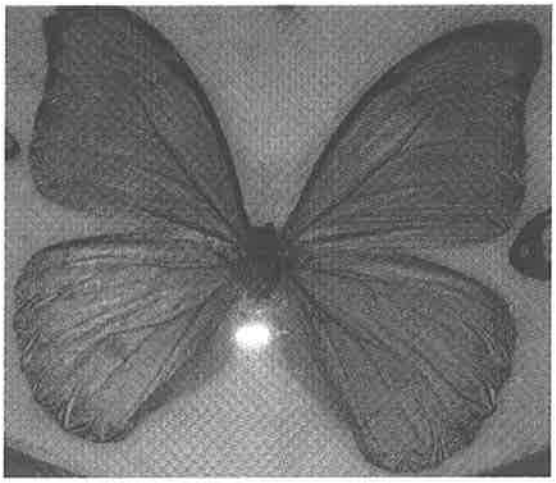

図 2: 構造色を呈するモルフォ蝶の翅

ルフォ蝶の翅をはじめとして, コガネムシの翅, カワセミや孔雀, 鴨, 鳩などの鳥のきらきらとした羽根は色素で色づいているのではなく, 鱗粉や翅, 羽毛の内部構造により光を反射し色を呈する, 構造色というものです. 法隆寺が所蔵する玉虫厨子のように構造色を用いた昆虫の翅で装飾すれば, 色素のように退色することがなく, 後世まで色を維持することができます. 真珠の輝きやオパールの色も構造色によるものです. 近年, 人工的に周期的に光を反射する構造（フォトニック結晶）を作り, 光の閉じ込めやフィルター, 光コンピュータに利用しようという研究が世界中で行われています.

これまでの例は電磁波（光）の例ですが, 電子（電子波）でも同じような現象が起こります. 原子が整然と並んだ結晶中では, 電子波が結晶原子により散乱されるため, 図 3 のように電子が存在できないエネルギーが生じます. 電子が存在できるエネルギー帯をエネルギーバンド, 電子が取れないエネルギー帯を禁制帯（エネルギーバンドギャップ）と言います. エネルギーバンドの構造やどの程度電子が詰まっているかによって, 金属, 半導体, 絶縁体の違いが生じます. 先ほどのフォトニック結晶は, 結晶の中の電子のアナロジー（類比）を光で実現しようとしているものである. 近年, 音波についても, フォノニック結晶として同様の研究がなされ, 吸音材などへの応用が期待されています. 地表を伝播する地震波でも同じような現象は起こります.

これらは波の干渉という現象を利用しています. 波動現象は定常的（絶え間なく波が同じようにお押し寄せてきている状態）には, Helmholtz 方程式という同じ（偏微分）方程式を満たします. したがって, 全ての波で同じようなことが期待できるのです.

この課題では, 実験もしやすいので水面波で考えてもらいました. 要するに, 水面波に対してレーダーのようなパラボラの反射板のような構造を考えればいいということになります.

電磁波の場合, 金属の棒, 網が波を反射, 散乱し, 干渉を起こさせます. 水面波の場合, 杭を等間隔に打つのもの一つの方法です. . 電子波の場合, あるエネルギーを持つ電子波が図 4 のように電子波が流れている導波路に 導波路を横断する方向にほぼ半波長の等間隔に 9 個散乱体を置き, それを波の進行方向に等間隔に 3 層並べると, 図 5 のように完全に反射されるようになる. これは, 導波路内では電子のエネル

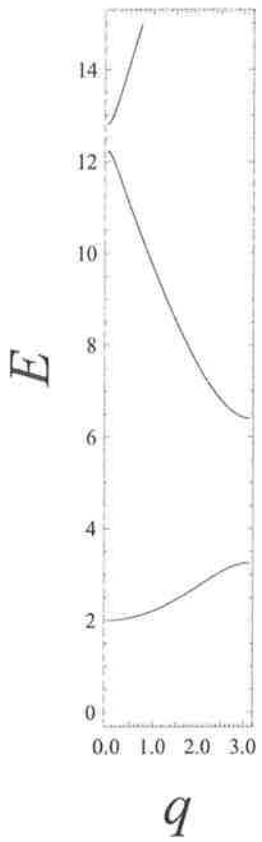

図 3: 電子のバンド構造（１次元系）

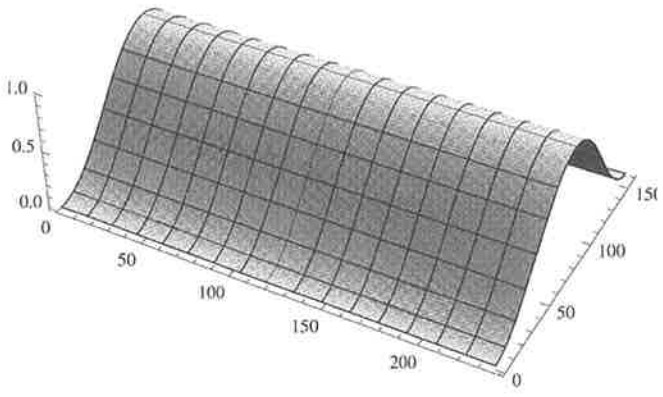

図 4: 導波路内の電子波（電子の存在確率）

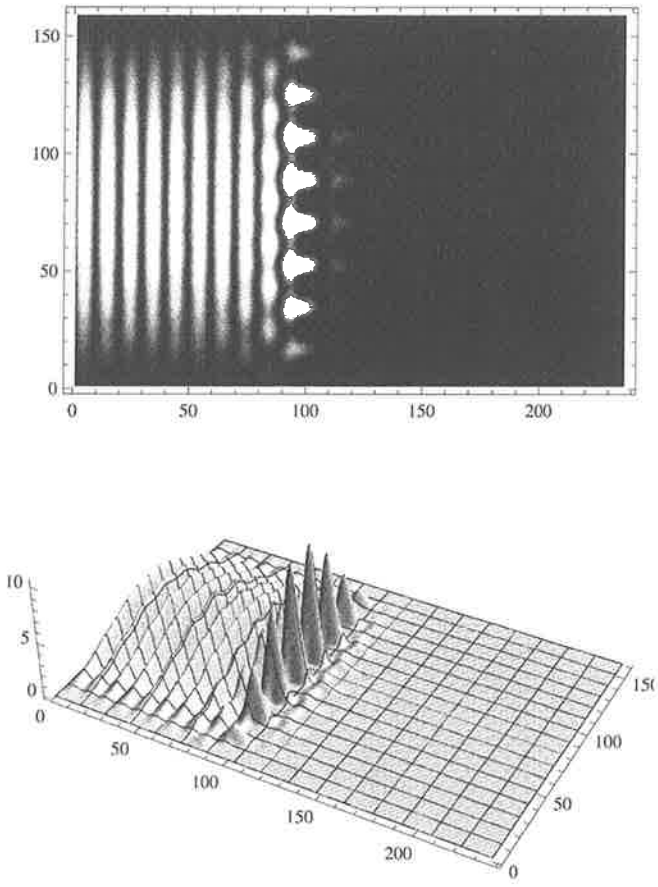

図 5: 導波路内に散乱体を横 9× 縦 3 の散乱体を並べた場合の電子波（電子の存在確率）

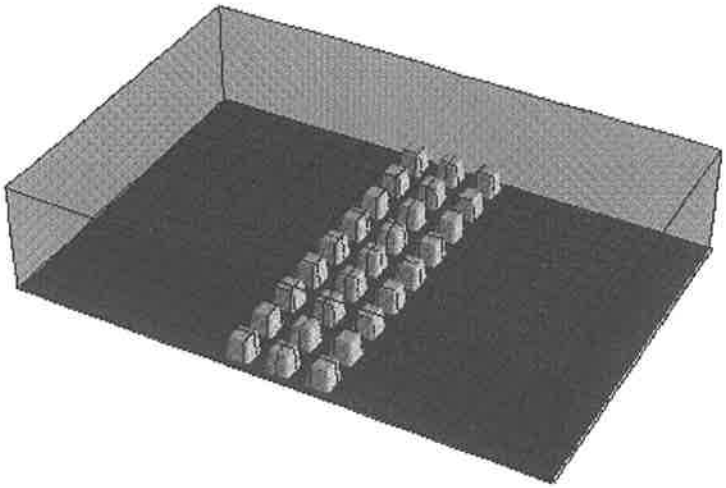

図 6: 海底に周期的凹凸を付けた干渉構造

ギーがバンド内にあり, 散乱体が周期的に並んだ場合にはバンドギャップ内にあるという解釈もできる. 水面波でも同様な現象が実現可能である. しかし, 波の波長により完全に反射されるようになる散乱体の周期は変わることに注意しなければならない. 課題文に「波の周波数（波長）は１種類として考えてください.」とあるのはそのためである.

さて, 海岸付近に杭を等間隔に打ってもよいが, 海面が白波を立て, 波が崩れるようになると杭に大きな力がかかり, 破壊される可能性がある. 水面に出ているよりも, 海底近くにある方が影響は少ない.

散乱体が水面に出ていなくても波の反射, 散乱は起こる. 波はその進行速度が変化する境界で反射, 屈折する. 水面波の伝播速度は深さの平方根に比例するから, 図 6 のように海底の高さを周期的に変化させると杭を等間隔で打ったのと同じ効果が得られます.

講評

課題には多くの参加者が取り組んでいたようですが, 実験をやっていたグループは単なる水遊びになってしまった例も少なくないようです.

答案には, 海岸に等間隔に杭を打つと答えたもの, 海底に周期的な凹凸をつけると答えたもなど鋭い洞察力の答案がありました. 「周期的」構造, 海底の深さを変化させるというポイントを押さえているものを高く評価しました. さらに, その構造で何故波が打ち消せるのか, 干渉についての考察まで行っているものありました. 素晴らしい答案だと思います.

波動現象は身近なところから, 最先端技術までいろいろなところに現れます. 光（電磁波）, 電子波（物質波）, 音波, 地震波など様々な波動現象がありますが, これらは基本的には統一的に取り扱えるのだということを心に留めておいてください.

2　課題2

課題

図 7(a), (b) のように, 互いに接する 3 つの円盤の作る隙間を大きさを変えながら常に 3 つの円に接するように配置して埋め尽くす問題は “Apollonian packing”(アポロンの敷詰め（詰込）) と呼ばれ, その起源は紀元前 200 年にさかのぼります. このような問題は地震の発生メカニズムとの関連で研究がされ

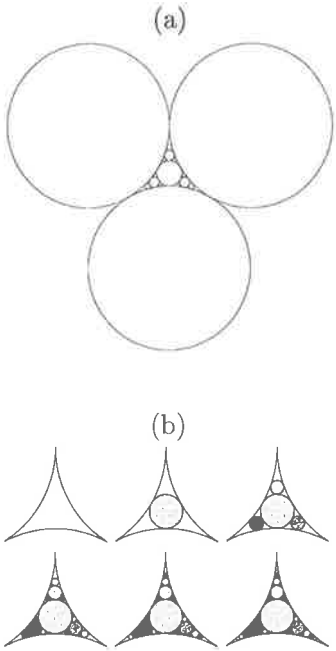

図 7: “Apollonian packing”(アポロンの敷詰め（詰込）) (a), 拡大 (b)

るようになっています. 地震が発生することなしに大陸（地面）の乗ったプレートが滑る現象があり, それは, 2 つの反対方向に動くプレートの間にプレートが崩れた様々な大きさの破片が挟まれているが, 破片がベアリングの役割をすることによってプレートが滑らかに滑るからではないかと考えられています.

さて, 今日はこの問題と関連して, 図 8 のように, 円筒内に数個の円柱をそれまでの世代の円柱に接するように置き, 残った隙間をより小さな円柱で同じことを繰り返し埋めていくことを考えます. そのとき, 円筒を回転させたとき, 全ての円柱が抵抗なく回転するにすることはできるでしょうか？ただし, 接した円柱, 円筒内壁は滑りなく, 互いに逆向きに回転するものとする. 可能であれば, どのような規則で配置すればよいか, その規則を見出してください. ただし, 円筒内に入れる最も大きな円柱の一つは円筒の内壁に接しているものとします.

解説

この課題は問題文にもあるように, もともと熱や地震を伴わない地殻プレートの滑りを説明するためにフランスの研究者たちにより研究された問題です. アメリカ物理学協会 (American Physical Society,

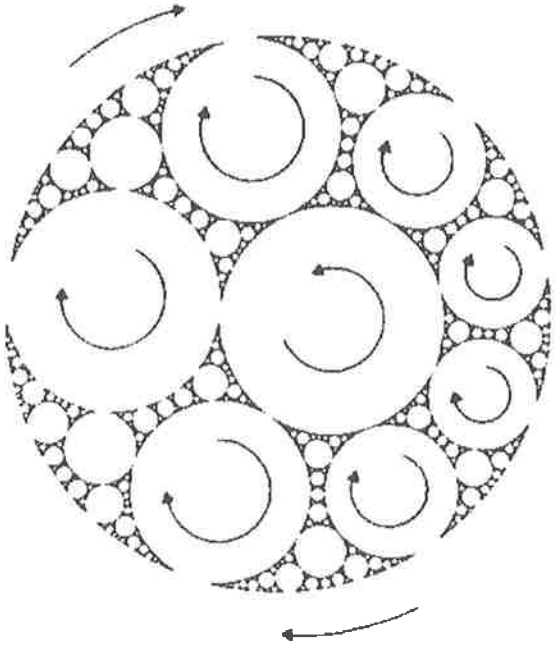

図 8: 円空間埋め尽くし回転円柱ベアリングの例

APS) 発行の世界の物理学会系論文誌の中で最も権威のある Physical Review Letters に掲載されています.

H. J. Herrmann, G. Mantica, and D. Bessis : "Space-Filling Bearings", Phys. Rev. Lett., Vol. 65, (1990) pp.3223-3226.

課題に示した図はこの論文からとったものです. そういう意味では, 課題文は「全ての円柱が抵抗なく回転するにすることはできるのか?」となっていますが, 一つの答えが出ているので必ずできるということです.

この問題について, Herrmann たちは一つの円柱が接した円柱がどのように回転するかから, 考察しています. 1 つの円柱に接する円柱は元の円柱の逆回りでなければならない. もし, 接した円がつながって閉じた輪を作るならば, その輪に含まれる円柱の数は偶数でなければならないという条件を示しています.

それを満たす階層構造を持つ図形を求めることは Coxeter 代数により実現できることを示し, それを用いて実際に作図しています. そのとき, 第 1 系列, 第 2 系列の 2 種の図形があり, 前者については以下のように描ける. 図 9 (a) のように下の直線 $\hat{\mathrm{C}}_0$ に接する半径 R_{B} の最大の円 (円 B) を描く, その円と上の直線 C_0 に同時に接する半径 R_{A} の円 (円 A) を描く. この時の 2 つの円の中心間の直線に沿った方向の距離を a とする. その後, 円 B の中心と $\hat{\mathrm{C}}_0$ との接点を通る軸に対する鏡像, 円 A の中心と直線 C_0 との接点を通る軸に対する鏡像, 円 B と $\hat{\mathrm{C}}_0$ との接点を中心とする半径 $r_{\mathrm{B}} \equiv \sqrt{2R_{\mathrm{B}}}$ の円の内 (外) 側を外 (内) 側に等角写像 (分数変換) する, 円 A と C_0 との接点を中心とする半径 $r_{\mathrm{A}} \equiv \sqrt{2R_{\mathrm{A}}}$ の円について分数変換するなど, 3 種のメビウス変換を繰り返し行うことにより 2 つの平行直線の間を隙間なく埋

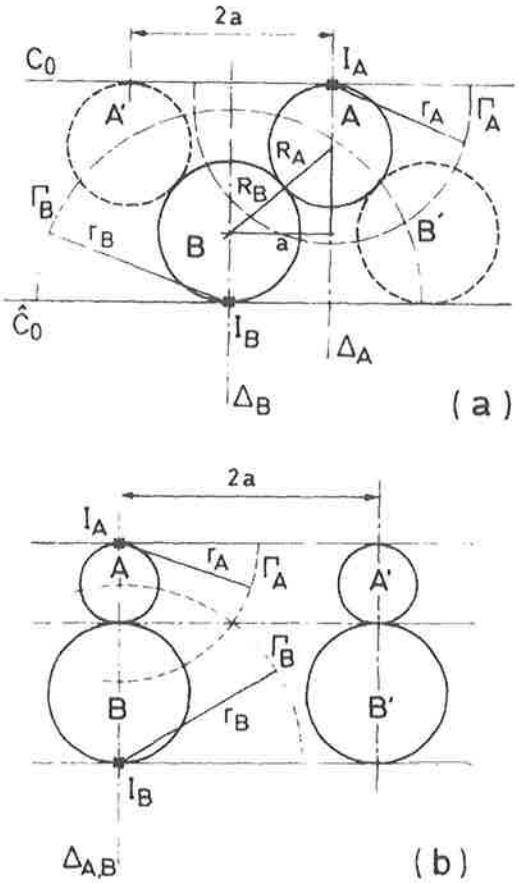

図 9: 2 平行直線間を円で充填する作図の初期状態の例 (a) 第 1 系列, (b) 第 2 系列

めることができる.

その結果, 図形は 2 つの整数 (n, m) で区別され, $z_n = \cos^{-1}[(\pi/(n+3))]$ として, a, r_{B}, r_{A} は

$$a^{-2} = z_n + z_m - 1,\ r_{\mathrm{A}}^2 = a^2 z_n,\ r_{\mathrm{B}}^2 = a^2 z_m$$

で与えられる.

第 1 系列の充填の様子をいくつか図 10 に示す.

第 2 系列については, 図 9 (b) のような図から始める. この場合も, このとき, 2 つの整数 (n, m) で区別され, a, r_{B}, r_{A} は

$$a^{-2} = z_n + z_m,\ r_{\mathrm{A}}^2 = a^2 z_n,\ r_{\mathrm{B}}^2 = a^2 z_m$$

で与えられる.

さて, これまで, 2 つの平行直線の間に円を詰める問題を考えてきたが, この課題は円の中に詰めるというものでした. そのためには, また, 等角写像を用います. 円 B について 2 平行直線の間の空間を円 B の中に移す等角写像をすれば, 円の中が完全に詰まった図形が得られます. $n = 4$, $m = 4$ の場合にそれを行たものが課題に示していた図です.

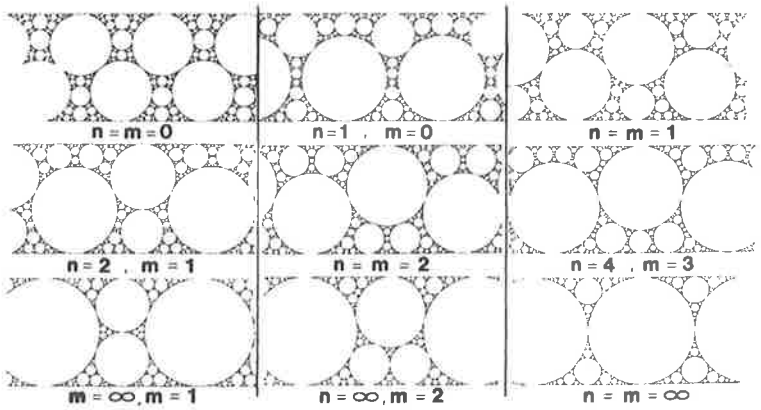

図 10: 2 平行直線間充填の第 1 系列の例

写像というと難しそうですが, 実は比較的身近な数学で, 普段使っている地図は地球の表面を長方形の平面に写像したものです. 映画もフィルム上の絵をスクリーンに写像（射影）したものです. 高校の数学でも行列を用いた写像（一次変換）を習いますが, 物理学においても写像（***変換）はよく現れます. 静止している人が観る現象と, 等速で移動している人が観るをつなぐガリレイ変換, 移動が光速に近くなった場合, 特殊相対性理論になり, ローレンツ変換が用いられます. また, 物体の運動（位置などの時間変化）も写像と考えることができます. 量子力学においては, 状態の時間発展や状態の回転, 平行移動, 全てがユニタリー変換で記述されます. また, 電磁気学で複雑な形の金属の周りの電位や電場を求めるときにはシュワルツ-クリストフェル変換というものが用いられます.

その基礎は高校の行列や一次変換にあるのでこのような分野に興味がある人はしっかり勉強しておいてください.

今回は 2 次元（円）で考えましたが, この問題は 3 次元の場合も考えられます. つまり, 大小の球を隙間なく詰めて抵抗なくスムーズに回すことができるのか?その研究もなされていて, 可能であることが R. Mahmoodi Baram, H. J. Herrmann, and N. Rivier : “Space-Filling Bearings in Three Dimensions”, , Phys. Rev. Lett., Vol. 92, (2004) 044301. に報告されています.

講評

この課題も多くの参加者が取り組んでくれました. 実際に構造を作って考察したもの, 紙に図を描いて考察したもの様々なアプローチで考察していました. 実験用に木の円柱, ビニールパイプの蓋, ストローなどいろいろ用意してはありました. 木の円柱は切って使うことを想定していましたが, 課題 1 の実験で丸ごとプールに放り込まれたようです. 紙を丸めて筒を作り実験していたグループもあり, 感心しました.

さて, 答案は様々試した苦悩と努力の跡が垣間見られるものが多数ありました. その中でも少なくない個人, グループが抵抗なく回転する条件「任意の閉じた曲線に沿って存在する円柱の数は偶数個」にたどり着いていました. これがこの問題を幾何学の問題にする出発点であるので, これにたどり着けたこ

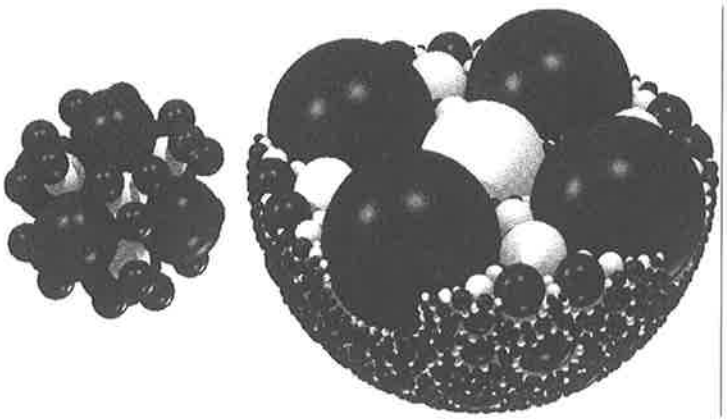

図 11: 球形ベアリングによる 3 次元空間充填の例

とは非常に重要で, 高く評価しました. 後は, これを数学的にどう表現するかですが, そこから先は高度な数学的問題なので, 興味があれば将来考えてみてください.

3　課題3

課題

ある問題を解くための基本的な計算の回数や, 計算を行う順序などを解析し, 計算方法の一般的法則を研究する分野を理論計算科学と呼びます. 理論計算科学で取り上げられる基本的な例題に「ハノイの塔」があります. ハノイの塔は以下の様に記述されます.

- 3 本の柱と, 柱が貫通する直径の異なる円盤が多数用意されている.
- ある柱に, ある枚数の円盤を下から上に向かって小さくなる様に配置する.
- このとき, 以下の規則ですべての円盤をほかの柱に移動する.
- 1 度に移動させる円盤は 1 つ.
- 移動中に, 常に下の円盤が大きくなる.

この問題を数学的に記述すると, 3 つの記憶領域　A, B, C を用意する. 領域 A にデータ $x_1, x_2, \cdots, x_n$ を記憶する. このとき, 処理途中にデータの順序を変えずに, すべてのデータを一ずつ動かして, 領域 B に移動させる. $n = 3$ のとき状態推移は以下の様になります.

A	B	C
$(1,2,3)$	$(\ ,\ ,\ )$	$(\ ,\ ,\ )$
$(\ ,2,3)$	$(\ ,\ ,1)$	$(\ ,\ ,\ )$
$(\ ,\ ,3)$	$(\ ,\ ,1)$	$(\ ,\ ,2)$
$(\ ,\ ,3)$	$(\ ,\ ,\ )$	$(\ ,1,2)$
$(\ ,\ ,\ )$	$(\ ,\ ,3)$	$(\ ,1,2)$
$(\ ,\ ,1)$	$(\ ,\ ,3)$	$(\ ,\ ,2)$
$(\ ,\ ,1)$	$(\ ,2,3)$	$(\ ,\ ,\ )$
$(\ ,\ ,\ )$	$(1,2,3)$	$(\ ,\ ,\ )$

代表的な解法は以下の 2 つです.

解法 1

1. 高さ $(n-1)$ の塔を A から C に移す.
2. n 番目の円盤を A から B に移す.
3. $(n-1)$ の塔を C から B に移す.

解法 2

以下の処理を交互に繰り返す

1. 最小の円盤を現在の柱から, 時計と同じ方向に動かす.

2. 円盤をやり取りする柱の対を反時計まわりに1ずつずらす.

さて, 映画「スタートレック」には未来の競技として, 3次元チェスが出てきます. また, 数学的興味から, チェスの板を六角形にしたものがあります. そこで, ハノイの塔の一般化とその解法を考えてください. たとえば, 柱の数を増やす, 柱を空間的に配置して柱間の移動の制限を加える. 円盤の移動制限を変える. などがあります. これらの場合, 一般的な解法を作ることができるでしょうか.

解説

多くの参加者が取り組んだ課題です. 解法1は再帰表現と呼ばれる解法の表現法です. また, 解法2は反復と呼ばれる表現法です. 与えられた問題の解法を形式的に表現し, その計算回数を評価することを取り扱う分野を理論計算機科学といいます. 再帰と反復は理論計算機科学の中で最も基本的な表現です. また, 問題によっては再帰を反復に変換することができます. ハノイの塔は再帰を反復に変換できる代表的な例です. ハノイの塔の一般化は多数存在します. しかし, 未解決の課題も多数あります. たとえば, 4つの塔の場合の最適解つまり, 最小移動回数も未解決問題の一つです.

講評

ハノイの塔の一般化として, 代表的なものは,

- 塔の数を増やす.
- 円盤に種類を付加する.
- 動きを制限する.
- ハノイの塔の存在する空間を変える. (たとえば、平面の裏表を考える)
- 上の4つを組み合わす.

です. 2つ以上の拡張を組み合わせることも考えられます. 今回, 新たに

- 競技者の数を増やす.

が追加されました. この拡張を学長賞としました. また、空間の変更と動きの制限を同時に行った拡張を学長賞としました.

4　課題 4

課題

高分子とは同じ構造を持った基本単位が一定の法則で繋がった構造体と考えることができます. 普通, 高分子は3次元空間に存在します. ここではまず, 2次元世界, すなわち, 平面上に存在する高分子の性質を解析することを考えます. 2次元世界の高分子は, 小さな円盤が接続してできた物体と考えることができます. 高分子は, 構成要素が一鎖や網目状に接続していますが, 要素が水を仲立ちとして接し合い縒れた糸の様になります. この性質を考慮して, たとえば分子のよじれに規則性を考慮したり, 枝別れに規則性を考慮すると, 実際の高分子の構造をモデル化できます. いろいろな条件を考えたときに, 高分子の基本要素の数と高分子の体積 (面積) と関係を見積もってください. 構成要素を正方形とすると, この見積もりはどうなりますか. また, 3次元ではどうなりますか. さらに, 円盤の半径や種類による接続構造を変えると, 面積, 体積の見積もりはどうなります.

解説

高分子を数理的に取り扱う場合, 格子点（座標値が整数の点）に構成要素を配置し, 点と点とを結ぶ線で構成要素を繋ぎます. ある点から出発して, 上下左右に等確率で接続を続けると高分子の骨格を近似することができます. 方向の自由度を増ためには, 同じ半径の円盤をつなげることを行います. さて, このような高分子のモデルで構成要素の個数を固定した場合に, たとえば, 次の様な疑問が生じます.

- 最大長を決めると, 最大いくつの分岐を許すことができるか.
- 分岐から分岐までの長さを固定すると, 高分子が占める最大面積はどうなるか.
- 規則的な折り曲げを考えると, 最大面積はどうなるか.

また逆に, 面積や長さ固定した場合には

- 最大いくつの分岐が許されるのか.
- 最大いくつの折り曲げが許されるのか.

などが問題になります. このような問題は高分子化学を外れて, 確立構造の問題になります.

講評

何を答えたらいいのかが難しかったのでしょう. あまり手を付けていませんでした. 高分子科学, さらに広く材料科学は, 物質を合成するや, 物質の物理的, 化学的性質を調べることが現在までは主流でした. しかし, 計算機の進歩により数理モデルを構築し, 構築したモデルに従って, 合成される物質の性質が予測できるようになってきました. このような分野では, 組合わせ解析や, 確率論が今まで以上に重要になっています. 対称性のある構造の面積を見積もった解答を学長賞としました.

5　ロボットの部

平成21年度22年度に開催したロボットの部は本年度はロボットへのサポートの停止により停止しました. 新たなロボットを利用して再開すべく, 用意をすすめています.

The graph for the Tower of Hanoi with four pegs

Man-Keun Lee

Dongyang University, Korea
email: mankeun@phenix.dyu.ac.kr

Introduction

The Tower of Hanoi is familiar to most mathematicians. The first solution to the Tower of Hanoi published in the mathematical literature appeared in 1884 in an article by Allardice and Fraser.

If we formulate the problem as one of determining the number of moves required to transfer a tower of n disks to three pegs, it is not difficult to solve. Indeed, this problem frequently appears as an elementary exercise in discrete mathematics textbooks. In its standard form, the puzzle consists of three numbered pegs and n disks. Initially, the disks, which have radius 1, 2, 3, ..., n are all placed on peg 1 in decreasing order of size such that the smallest disk is on top and the largest disk is at the bottom. A move of the puzzle consists of taking the top disk off one peg and moving it to another. A move is called legal if it does not involve covering a smaller disk with a large one. The object of the puzzle is to transfer all of the disks from peg 1 to one of the other two pegs, using only legal moves. We are interested in the optimal solution to the puzzle, that is the minimum number of legal moves required to move the disks from one peg to another. If we let h_n denote the number of moves required to transfer a tower of n disks from one peg to another, it is easy to see that we first move the top n-1 disks from the initial peg to an intermediate peg, then the largest disk to the target peg, and finally the n-1 disks from the intermediate peg to the target peg. This gives us the recurrence relation:

$$h_n = 2h_{n-1} + 1, \quad h_1 = 1$$

By solving the recurrence relation we find the well-known solution:

$$h_n = 2^n - 1$$

This h_n is the optimal solution to the puzzle (Wood, 1981).

Perhaps the greatest challenge is posed by increasing the number of pegs. The modification is to change the number of pegs from 3 to t, where $t \geq 2$. The purpose and the rules of this modified version are the same as the standard one. The reason why this puzzle is interesting at all is that the optimal solution to the puzzle is not unique, and it is not obvious how to derive a solution. A method for achieving optimal splitting of a tower of n disks appears to be more complicated than one would initially imagine. To gain a more intuitive understanding of the principles involved, we will discuss a step-by-step derivation that eventually leads to the optimal method.

Before this discussion, let us tabulate the minimum number of disk moves for each combination of t pegs and n disks. This gives us Table 1.

n	t=2	t=3	t=4	t=5	t=6	t=7	t=8
0	0	0	0	0	0	0	0
1	1	1	1	1	1	1	1
2		3	3	3	3	3	3
3		7	5	5	5	5	5
4		15	9	7	7	7	7
5		31	13	11	9	9	9
6		63	17	15	13	11	11
7		127	25	19	17	15	13
8		255	33	23	21	19	17
9		511	41	27	25	23	21
10		1023	49	31	29	27	25
11		2047	65	39	33	31	29
12		4095	81	47	37	35	33
13		8191	97	55	41	39	37
14		16383	113	63	45	43	41
15		32767	129	71	49	47	45
16		65535	161	79	57	51	49
17		131071	193	87	65	55	53
18		262143	225	95	73	59	57
19		524287	257	103	81	63	61
20		1048575	289	111	89	67	65

Table 1

Let M(t, n) be the minimum number of disk moves in transferring a tower of n disks from one peg to another using all t pegs. From Table 1, we obtain

$$M(t,n)=\sum_{i=0}^{k-1}2^i\left(\frac{t-3+1}{t-3}\right)+2^x\left[n-\left(\frac{t-3+x}{t-2}\right)\right]$$

where x satisfies

$$\left(\frac{t-3+x}{t-2}\right)\le n<\left(\frac{t-2+x}{t-2}\right)$$

This was deduced by M. C. Er (1988).

In this paper, we will take another approach to the Tower of Hanoi problem. Using only elementary ideas from graph theory, we will establish a correspondence between configurations of disks arising in the Tower of Hanoi problem and a fractal. We will then use this correspondence to solve a Tower of Hanoi with 4 pegs. A very interesting development in this direction can be found in Stewart (1992). The starting point of this paper is the observation of Stewart's method, which we elaborate on in Section 2.

The Tower of Hanoi graph

Consider the Tower of Hanoi with just three disks. To construct the graph, we must first find a way to represent all possible positions, then work out the legal moves between them, and finally draw up the graph. We number the three disks 1, 2, 3 with 1 being the smallest and 3 the largest. We number the pegs 1, 2, 3 from left to right (see Figure 1).

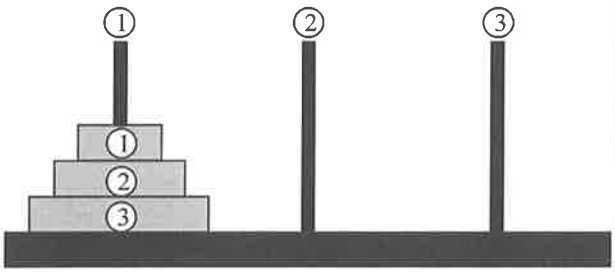

Figure 1

For example, if disk 1 is on peg 2, disk 2 is on peg 1, and disk 3 is on peg 2, then we have completely determined a potential position. We can encode this information in the sequence 212, the three digits in turn representing the pegs for disks 1, 2 and 3. Therefore each position in a 3-disk Tower corresponds to a sequence of three digits, each being 1, 2 or 3.

It follows that there are precisely $3^3=27$ different positions in a 3-disk Tower of Hanoi. Indeed, by using the graph it is clear that we can get from any position to any other, and it is also clear what the quickest route is.

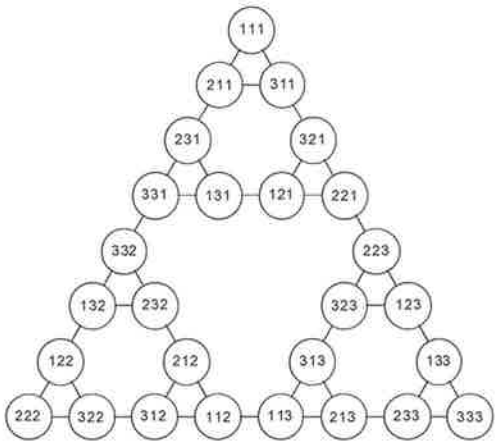

Figure 2: Graph for three-disk, three-peg tower

The graph (see Figure 2) consists of three copies of a smaller graph linked by three single edges to form a triangle. Each smaller graph in turn has a similar triple structure. Similarly, the graph for a 4-disk Tower of Hanoi consists of three copies of a 3-disk graph linked at the corners like a triangle. Using the same argument, we can say that the Tower of Hanoi has a recursive structure; the solution to an (n+1)-disk Hanoi is determined by that for an n-disk Hanoi according to a fixed rule. As the number of disks becomes larger, the graph becomes more and more intricate, looking more and more like the Sierpinski gasket. This shape is fractal-like.

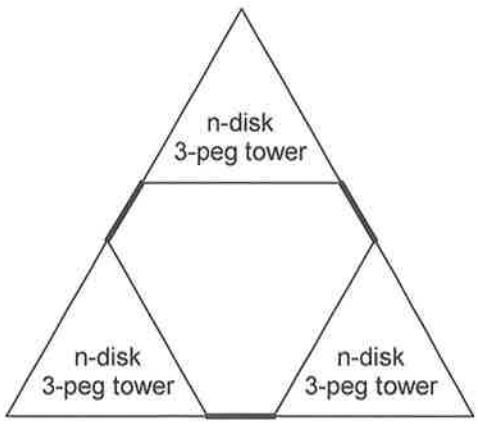

Figure 3: The graph for an (n+1)-disk three-peg tower

Looking at Figure 3, we can see that the number of vertices along a side of the graph doubles at each stage, and is 2^n for an n-disk Hanoi. The number of edges along a side (which is what we want) is

one less than this, namely $2^n - 1$. Suppose there are e_n edges in the n-disk graph. The recursive structure implies $e_{n+1} = 3e_n + 3, \quad e_1 = 3$.
Thus we get the following proposition:

PROPOSITION: For an n-disk (3-peg) Tower of Hanoi, the minimum number of moves needed to move all n disks from one peg to another is $2^n - 1$ and the total number of distinct moves from one position to another position is $3^{n+1} - 3$.

The graph for a Tower of Hanoi with four pegs

Consider first a 1-disk 4-peg Tower. There are clearly only three different possible moves. The graph of this situation can be represented by a tetrahedron in 3-dimensional space (see Figure 4).

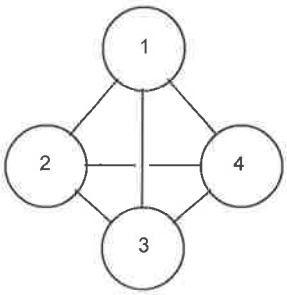

Figure 4: The graph for the one-disk, four peg problem

We continue with 2 disks and a four-peg tower. With 2 disks and 4 pegs, there are precisely 4×4=16 different positions. We can list all these 16 positions and all possible moves by following the legal moves. The result is shown in Figure 5.

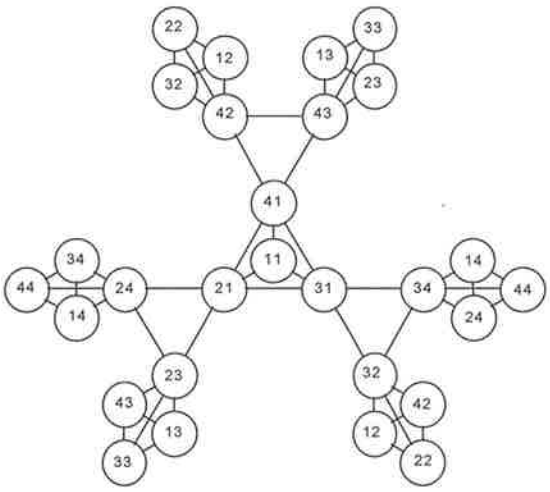

Figure 5: Graph for two-disk, four-peg problem

The next task requires care and accuracy, but little thought. After many attempts, we can rearrange the vertices and edges to avoid overlaps. Drawing the graph in 3-dimensional space leads to Figure 6. The graph resembles a tetrahedron.

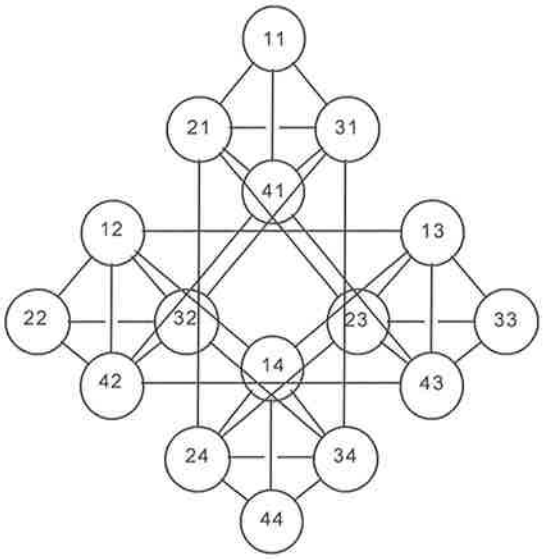

Figure 6a: The connection of each point

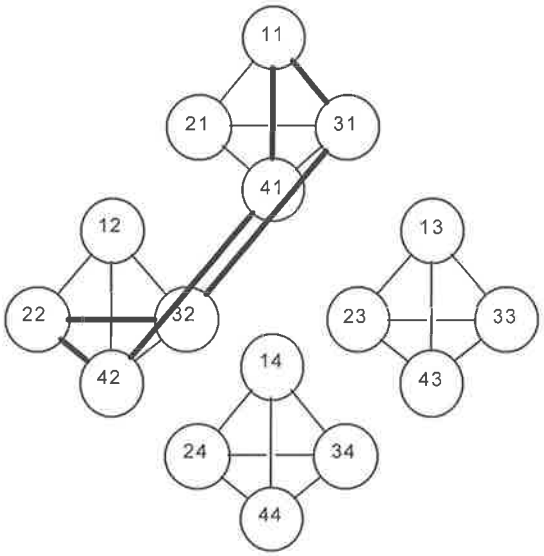

Figure 6b: The two shortest paths to move the two disks from peg 1 to peg 2

To transfer both disks from peg 1 (position 11) to peg 2 (position 22) we merely run down the edge, making the moves:

$11 \rightarrow 41 \rightarrow 42 \rightarrow 22$,
or $11 \rightarrow 31 \rightarrow 32 \rightarrow 22$ (see Figure 6b).

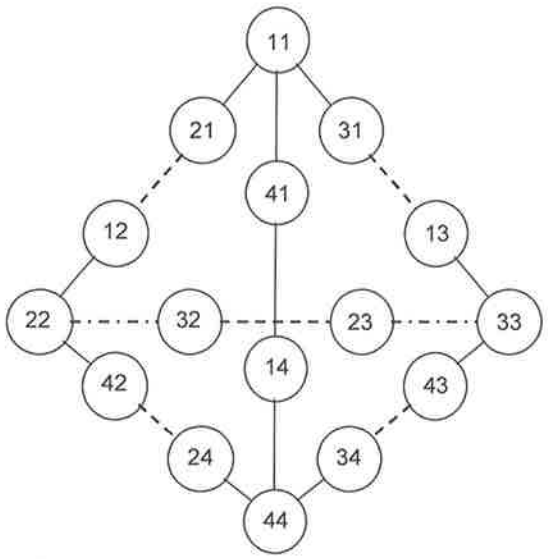

Figure 6c: Each position of the graph shown on a tetrahedron

As indicated previously, by consulting the graph it is clear that we can get from any position to any other, as well as what the quickest route is. The graph consists of four copies of a smaller graph, linked by 12 edges to form a tetrahedron. In this graph, we also find that the following graphs are all rectangles:

21-41-43-23-21,
41-31-32-42-41,
21-31-34-24-21,
12-13-43-42-12,
12-14-34-32-12,
14-13-23-24-14.

The same argument works for any number of disks. The graph for a 3-disk Hanoi with four pegs, for example, consists of four copies of the 2-disk graph, linked at the corners like a tetrahedron (see Figure 7). So we can say that Tower of Hanoi with four pegs has a recursive structure and the graph again resembles a fractal.

Figure 7 shows the graph for a 3-disk Tower of Hanoi, drawn by applying this recursive structure. Without this graph, it would take days to work out a 3-disk Tower of Hanoi by listing all $4^3 = 64$ possible positions and finding all the moves between them (and one would probably make several mistakes along the way).

In Figure 8 we see that the number of vertices along a side of the graph doubles at each stage and is thus 2^n for an n-disk Hanoi with four pegs. This means that the graph for an n-disk Hanoi with four pegs consists of four copies of the (n-1)-disk graph, linked by 6.2^{n-1} edges to form a tetrahedron. So this graph is a fractal.

References

ALLOUCHE, J. P., ASTOORIAN, D., RANDALL, J. & SHALLIT, J., 1994, "Morphisms, Squarefree Strings, and the Tower of Hanoi Puzzle" in *American Mathematics Monthly*, **101**, pp. 651-658

ER, M. C., 1988, "An Optimal Algorithm for Reve's Puzzle" in *Information Sciences*, **45**, pp. 39-49

POOLE, D. G., 1994, "The Tower and Triangles of Professor Claus" in *Mathematics Magazine*, **67**, pp. 323-344

STEWART, I., 1992, *Another Fine Math You've Got Me Into*, W. H. Freeman and Company

WOOD, D., 1981, "The Tower of Brahma and Hanoi Revisited" in *The Journal for Recreational Mathematics*, **14**, pp. 17-24

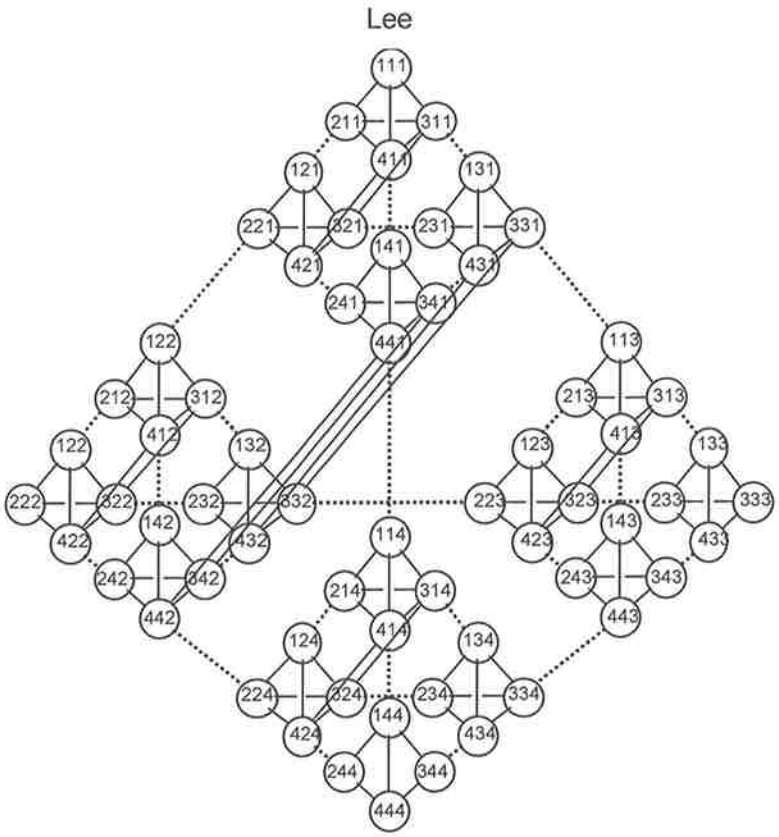

Figure 7: Graph of the 3-disk, 4-peg Tower of Hanoi (with only some of the routes shown)

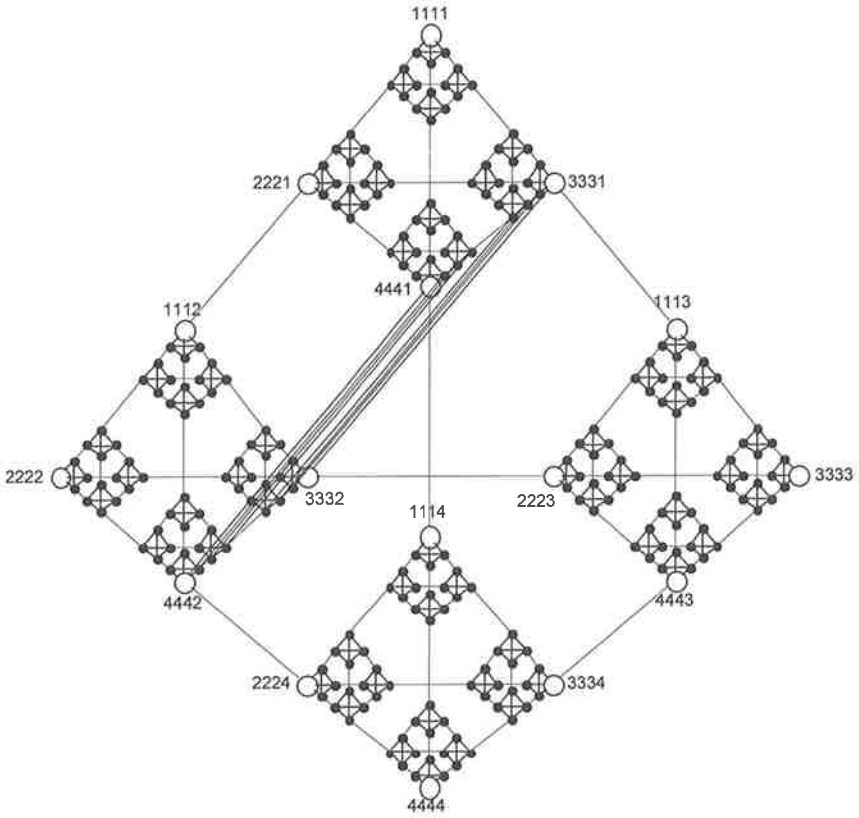

Figure 8: Graph of a 4-disk, 4-peg Tower of Hanoi (highlighting the fractal-like structure)

Branched Polymers

Richard Kenyon and Peter Winkler

1. INTRODUCTION. A **branched polymer of order** n in $\mathbb{R}^D$—or just "polymer" for short—is a connected set of n labeled unit spheres with nonoverlapping interiors. We will assume that the sphere labeled 1 is centered at the origin. See Figure 1 for an example in the plane.

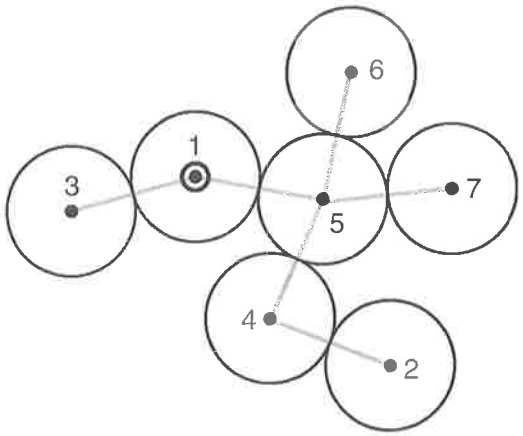

Figure 1. A branched polymer in the plane.

Intended as models in chemistry or biology, branched polymers are often modeled, in turn, by lattice animals (trees on a grid); see, e.g., [**3, 5, 8, 10, 18, 19**]. However, continuum polymers turn out to be in some respects more tractable than their grid cousins.

In order to study the behavior of branched polymers, and in particular to define and understand what random examples look like, we must define a parametrization and then attempt to compute, using that parametrization, volumes of various configuration spaces. In principle, we could then compute (say) the probability that a branched polymer of a particular size in a given dimension takes the form of a specific tree, or has diameter exceeding some number; and we could perhaps generate uniformly random examples in an efficient manner.

Fortunately, the space of branched polymers of order n and dimension D possesses an obvious and natural parametrization. One of several equivalent ways to describe it is to specify the tree-type of the polymer, together with the $n-1$ D-dimensional angles at which each ball is attached to the next ball on the way to the root. This causes an ambiguity if the polymer contains a cycle of touching balls (thus has multiple spanning trees), but such polymers will have probability zero, so we don't mind if they are parametrized in more than one way.

For example, in the plane, the set of polymers with two balls (disks) is parametrized by a single angle at the origin (center of ball 1), measured counterclockwise from the x-axis to the center of ball 2. The volume of the configuration space is thus 2π.

For polymers of order 3, two angles are required: the first is the angle made by the lowest-numbered ball touching ball 1, and the second is the angle made by the center of the third ball to the center of the ball it touches. If ball 1 touches both other balls, then there are 2π's worth of possibilities for the location of ball 2. Once ball 2 has been placed, the angle of ball 3 is restricted to an interval of length $4\pi/3$ so as not to overlap ball 2.

One can measure the volume of the configuration space in terms of these angles, giving $(2\pi)(4\pi/3)$ for this configuration (which is one of three symmetric configurations, the others having ball 2 or ball 3 in the middle). The total volume for polymers of order 3 is then $8\pi^2$.

For higher-order polymers, different tree-types will have differing volumes, as well as differing numbers of symmetries. Figure 2 shows the various different topological types of configurations with 3, 4, and 5 balls, along with their respective volumes (in the plane). Remarkably, in dimensions 2 and 3 the sum of the volumes over all the n-ball configurations is an integer multiple of $(2\pi)^{n-1}$. Indeed, Brydges and Imbrie [**2**] showed that the space $B^D(n)$ of polymers of order n has total volume $(n-1)!\,(2\pi)^{n-1}$ for $D = 2$ and $n^{n-1}(2\pi)^{n-1}$ for $D = 3$. Their proof uses nonconstructive techniques such as equivariant cohomology and localization.

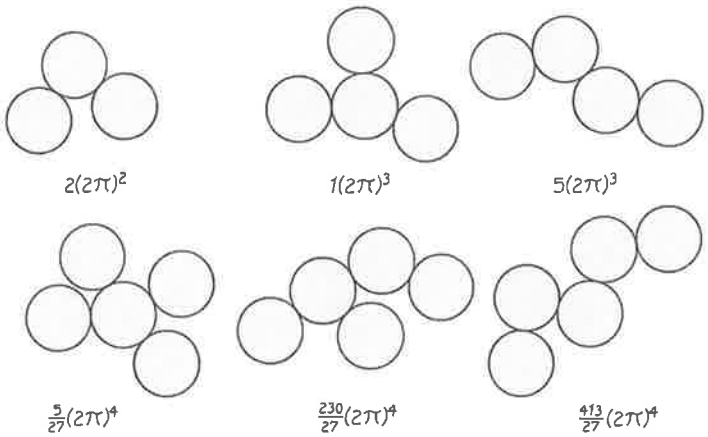

Figure 2. Branched polymers in the plane with 3, 4, and 5 balls, and the volumes of the corresponding configuration spaces.

We give here an elementary proof, together with some generalizations and an algorithm for exact random sampling of polymers. In the planar case our algorithm has the added feature of being inductive, in the sense that a uniformly random polymer of order n is constructed from one of order $n-1$.

Although it is not explicit in the paper, the proof in [**2**] in fact shows that in the planar case the volume of the configuration space is unchanged when the radii of the individual disks are different. We will prove this fact, which we call the "Invariance Lemma," and use it in our constructions. Along the way, we provide an easy proof for the notorious "random flight" theorem of Rayleigh and Spitzer. Moving to three dimensions, our development leads to both a random construction and a theorem about the expected diameter.

Our plan is as follows. In Section 2 we state the Invariance Lemma and use it to compute the configuration volume in two dimensions. In Section 3 we generalize to graphs, and apply the result to random flights. Section 4, devoted to 3-dimensional

polymers, uses the earlier results to compute volumes and diameter. Section 5 contains the proof of the Invariance Lemma. Sections 6 and 7 show how to generate uniformly random branched polymers in dimensions two and three. Finally, Section 8 gives some open problems.

2. THE PLANAR CASE. Let us observe first that $(n-1)!\,(2\pi)^{n-1}$ is also the volume of the space of "crossing worms"—that is, strings of labeled touching disks, beginning with disk 1 centered at the origin, but now with no overlap constraint. See Figure 3 for an example. Fixing the order of disks 2 through n in the crossing worm yields an ordinary unit-step walk in the plane of $n-1$ steps, whose configuration volume is just $(2\pi)^{n-1}$; the $(n-1)!$ ways to order disks 2 through n provide the additional factor.

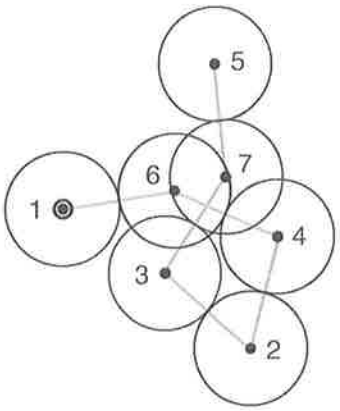

Figure 3. A crossing worm.

Another space of volume $(n-1)!\,(2\pi)^{n-1}$ is the space of "crossing inductive trees," one of which is illustrated in Figure 4. A crossing inductive tree is a tree of n touching labeled disks with overlapping permitted, but required to satisfy the condition that for each $k < n$, disks $1, \ldots, k$ must also form a tree. In other words, the vertex labels increase from the root 1. The configuration volume is verified easily by induction; a crossing inductive tree with $n+1$ disks is obtained by adding a single disk to an

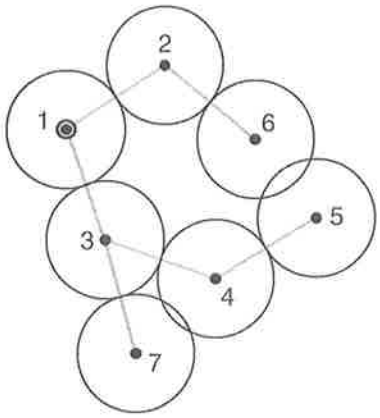

Figure 4. A crossing inductive tree.

already-constructed crossing inductive tree on n disks. To do this one of the n already-placed disks is chosen to add the new disk to, as well as a random point on its boundary, altogether multiplying the old configuration volume by $n(2\pi)$. We will see that this space is in fact a certain limiting case of the space of polymers.

Invariance. In this subsection we will state the critical Invariance Lemma; its proof (via multivariate calculus) will be postponed until later.

Let us consider 2-dimensional polymers made of disks of arbitrary radius. In particular let $r_i \in (0, \infty)$ be the radius of the ith disk, and $R = (r_1, \ldots, r_n)$ the vector of radii. Given a polymer $X = X(R)$, define a graph $H(X)$ with a vertex for each disk's center and an edge between vertices whenever the corresponding disks are adjacent. As before $H(X)$ is almost surely a tree, that is, has no cycles. When $H(X)$ is a tree, we root $H(X)$ at the origin, and direct each edge away from the origin. This allows us to assign an "absolute" angle (taken counterclockwise relative to the x-axis) to each edge, and to parametrize our R-polymer with these angles as we did for the unit-disk polymers above.

The choice of R may have a huge effect on the configuration volume for a given tree; for example, a tree having a vertex of degree greater than six cannot occur at all in the unit-disk case, but may have substantial volume when the radii vary widely. However, we have the following fact:

Lemma 1 (Invariance Lemma). *The total volume of the space of branched polymers of fixed order in the plane does not depend on the radii of the disks.*

What happens, as the proof (in Section 5) will show, is that as the radii change, volume flows from one tree to another through the boundary polymers (which have cycles), but is always preserved.

Let us use the Invariance Lemma to show that the constant volume in fact takes the claimed value.

Theorem 2. *For any radius vector R of length n, the volume of the space of branched polymers is $(n-1)!\,(2\pi)^{n-1}$.*

Proof. For the sake of readability we give an informal argument here, but one which can be made rigorous in a straightforward manner. Choose $\varepsilon > 0$ very small and let R be given by $r_i = \varepsilon^i$. Let X be a uniformly random configuration of disks with these radii, forming some labeled tree T. Suppose that for some $j < n$, disks 1 through j are connected. Then we claim that with probability near 1, disk $j+1$ touches one of disks 1 through j. To see this, observe that otherwise disk $j+1$ is connected to some previous disk i, $1 \le i \le j$, via a chain of (relatively) tiny disks whose indices all exceed $j+1$. Let disk k, $k > j+1$, be the one that touches disk $j+1$; then the angle of the vector from the center of disk k to the center of disk $j+1$ is constrained to a small range, else disk $j+1$ would overlap disk i. It follows that the configuration space for polymers of shape T and radii R has lost almost an entire degree of freedom. Thus, it has very small volume; in other words, the tree T is very unlikely.

Suppose, on the other hand, that for every j, disks 1 through j are connected. Then we may think of X as having been built by adding touching disks in index order, and since each is tiny compared to all previous disks, there is almost a full range 2π of angles available to it without danger of overlap.

It follows that as $\varepsilon \to 0$ the volume of the space of polymers with radius vector R approaches the volume of the space of crossing inductive trees, namely $(n-1)!\,(2\pi)^{n-1}$. Since this volume does not depend on R, we have equality. ∎

3. GENERALIZATION TO GRAPHS. We discuss now a more far-reaching generalization of planar branched polymers, which continues to exhibit the gratifying behavior above, and will be needed when we move to dimension three.

Let G be a graph on vertices $\{1, \ldots, n\}$ in which each edge $\{i, j\}$ is equipped with a positive real length r_{ij}. We call a subgraph H of G a *connector* if it contains a spanning tree, in other words, if it is connected and contains all the vertices of G.

A *G-polymer* is a configuration of points in the plane, also labeled by $\{1, \ldots, n\}$, such that:

1. point number 1 is at the origin;
2. for each edge $\{i, j\}$ of G, the distance $\rho(i, j)$ between points i and j is at least r_{ij}; and
3. the edges $\{i, j\}$ for which $\rho(i, j) = r_{ij}$ constitute a connector of G.

For a given spanning tree T, we let $\mathrm{BP}_G(T)$ denote the set of G-polymers such that for every edge $\{i, j\}$ of T, $\rho(i, j) = r_{ij}$.

Note that if G itself is not connected, then there are no G-polymers. If $R = (r_1, \ldots, r_n)$, and G is the complete graph K_n with $r_{ij} = r_i + r_j$, then a G-polymer is precisely the set of centers of the disks of a polymer with radius vector R, in the sense of the previous sections. The volume V_G of the space of G-polymers is defined as before by the angles made by the vectors from i to j, where $\{i, j\}$ is an edge for which $\rho(i, j) = r_{ij}$.

In fact, the proof of Lemma 9 extends without modification to show that V_G does not depend on the lengths r_{ij} (even if they fail to satisfy the triangle inequality), but only on the structure of G. This leaves us with the question of computing V_G for a given graph G.

To do this, we label the edges of G arbitrarily as $e_1, \ldots, e_m$, and if $e_k = \{i, j\}$ we let its edge length r_{ij} be 2^{-k}. Then, for the volume of $\mathrm{BP}_G(T)$ to be nonzero, there must not be an edge e_k of $G \setminus T$ such that k is the lowest index of all edges in the cycle made by adjoining e_k to T (the triangle inequality would cause e_k to violate condition (2) above). If no such edge exists we say that T is "safe"; in that case condition (2) can *never* be violated. Thus, when T is safe, the volume of the space of configurations in $\mathrm{BP}_G(T)$ is the full $(2\pi)^{n-1}$.

It follows that the volume of the space of *all* G-polymers is $\mu(G)(2\pi)^{n-1}$, where $\mu(G)$ is the number of safe spanning trees of G. Since the volume does not depend on the edge labeling, neither does $\mu(G)$. One might suspect therefore that $\mu(G)$ has a symmetric definition, and indeed it does.

Lemma 3. *For any graph G (and any numbering of its edges), the number $\mu(G)$ of safe spanning trees of G is equal to the absolute difference between the number of connectors of G with an odd number of edges, and the number of connectors of G with an even number of edges.*

Proof. The sum of $(-1)^{|H|}$ over connectors H of G is in fact $\mathcal{T}_G(1, 0)$, where $\mathcal{T}_G$ is the Tutte polynomial of G (see, e.g., [**1, 4, 17**]); we need to show therefore that $\mu(G) = |\mathcal{T}_G(1, 0)|$.

A simple inclusion-exclusion argument suffices. Let us fix a numbering of the edges of G and, for each spanning tree T, let $B(T)$ be the set of "bad" edges of $G \setminus T$, that is, edges which boast the lowest index of any edge in the cycle formed with T. Associate to each connector H the spanning tree $T(H)$ obtained from H by successively removing the lowest-indexed (i.e., longest) edge whose removal does not disconnect H. ($T(H)$ can also be defined as the spanning tree of H of least total length.)

We claim that for any spanning tree T, the connectors H for which $T(H) = T$ are exactly those of the form $T \cup S$ for $S \subseteq B(T)$. Indeed, if H is of that form, then the longest edge in S will be in a cycle (thus removable); any longer edge of H cannot be removable because for it to be in a cycle, an even longer edge from $B(T)$ would have to have been added. On the other hand, if H contains T and some edge e not in $B(T)$, the longest edge in the unique cycle in $T \cup \{e\}$ is some edge $f \in T$; that edge would be removed before e in the construction of $T(H)$.

Let n be the number of vertices of G; a spanning tree has $n - 1$ edges. Suppose first that n is odd. Then

$$\sum_H (-1)^{|H|} = \sum_T \sum_{S \subseteq B(T)} (-1)^{|S|},$$

but $\sum_{S \subseteq B(T)} (-1)^{|S|} = 0$ unless $B(T)$ is empty. Thus, the right-hand side of the equation is just the number of safe spanning trees, $\mu(G)$. For n even, we have

$$\sum_H (-1)^{|H|} = \sum_T \sum_{S \subseteq B(T)} (-1)^{|S|+1}$$

and both sides are now equal to $-\mu(G)$. ∎

Comparing with Theorem 2, we have indirectly shown that $\mathcal{T}_{K_n}(1, 0) = (-1)^{n-1}(n-1)!$. We note also that $\mathcal{T}_G(1, 0)$ plays the role of Brydges and Imbrie's function J_G in the dimension-2 case.

We summarize:

Theorem 4. *The volume of the space of G-polymers in the plane is $|\mathcal{T}_G(1, 0)|(2\pi)^{n-1}$.*

The precise computation of $\mathcal{T}_G(1, 0)$ is unfortunately #P-hard (thus, not possible in polynomial time assuming P $\neq$ NP) for general G [**7**]. The point $(1, 0)$ is not, however, in the region of the plane in which Goldberg and Jerrum [**6**] have recently shown the Tutte polynomial to be hard even to approximate. Thus, there is some hope that a "fully polynomial randomized approximation scheme" can be found for $\mu(G)$. Luckily, in this work, the graphs for which we will later need to calculate $\mathcal{T}_G(1, 0)$ are very special.

We conclude this section with a new solution of a notoriously difficult puzzle that appears as an exercise in Spitzer's book *Principles of Random Walk* [**14**, p. 104], and was derived from Rayleigh's investigation (see [**20**, p. 419]) of "random flight." The exercise calls for proving the corollary below by developing the Fourier analysis of spherically symmetric functions, then deriving a certain identity involving Bessel functions. Curiously, it is (we believe) the only mention of random walk in *continuous* space in the entire book.

Corollary 5. *Let W be an n-step random walk in $\mathbb{R}^2$, each step being an independent uniformly random unit vector. Then the probability that W ends within distance 1 of its starting point is $1/(n + 1)$.*

Proof. The volume of the space of such walks, beginning from the origin, is of course $(2\pi)^n$; these walks are just the "crossing worms" defined earlier, but with $n + 1$ disks. If the walk does *not* terminate inside the unit disk at the origin, it is in effect a C_{n+1}-polymer, where C_{n+1} is the $(n + 1)$-cycle in which vertex i is adjacent to vertex $i + 1$, modulo $n + 1$. In fact the walk is a C_{n+1}-polymer in which balls 1 and $n + 1$ are

not adjacent. Since $\mu(C_{n+1}) = |1 - (n+1)| = n$, the volume of the space of C_{n+1}-polymers is $n(2\pi)^n$. Since the spanning tree with no edge between nodes 1 and $n+1$ is one of $n+1$ symmetric choices, the volume of the C_{n+1}-polymers which correspond to non-returning random walks is $n(2\pi)^n/(n+1)$, and the result follows. ■

4. THE 3-DIMENSIONAL CASE

Volume invariance. Branched polymers in 3-space share many of the features of planar branched polymers. Brydges and Imbrie showed in [**2**] that the volume of the configuration space of polymers in 3-space is $n^{n-1}(2\pi)^{n-1}$. Here the volume is measured in terms of the spherical angles, that is, the surface area measure on the spheres. Whereas the planar configuration space volume was independent of the radii of the balls, the same is not true in 3 dimensions.

One-dimensional projections. Let X be a branched polymer in $\mathbb{R}^3$ with ball centers $v_1, \ldots, v_n$. It will be convenient to assume that spheres of which our polymers are composed have *diameter* 1 instead of radius 1; thus the distance between any two sphere centers is at least 1, with equality in a spanning tree.

Recall (a fact attributed to Archimedes) that if I is an interval on a diameter of a sphere, then the area of the surface of the sphere that projects onto I is 2π times the length of I. It follows that for the purpose of computing the volume of the configuration space, we may assume that the polymers are parametrized by the x-coordinates of the points $v_1, \ldots, v_n$, together with the angle to the positive y-axis of the projection of $v_i - v_j$ onto the yz-plane for each pair $\{i, j\}$ of adjacent balls.

Let $x_1, \ldots, x_n$ be the projections of $v_1, \ldots, v_n$ to the x-axis. We suppose, after relabeling if necessary, that the x_i are ordered $x_1 < x_2 < \cdots < x_n$ (we will ignore the nongeneric cases when two of the x_i's are equal). It will also be convenient to shift the x-coordinates so that $x_1 = 0$. If v_i and v_j are adjacent in the polymer then $|x_i - x_j| \leq 1$. (See Figure 5.) In other words, if $|x_i - x_j| > 1$, then the spheres of diameter 1 centered around v_i and v_j cannot touch, so their projections onto the yz-

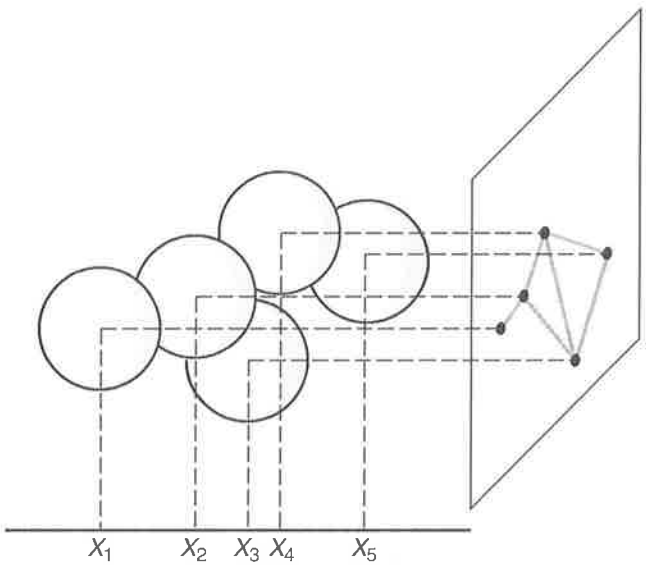

Figure 5. A branched polymer projected onto the x-axis and yz-plane.

plane are unconstrained. If $|x_i - x_j| \le 1$ then the yz-projections of v_i and v_j cannot be too close, else the corresponding spheres would overlap.

It follows that once $x_1 < x_2 < \cdots < x_n$ are fixed, the allowable projections of the sphere centers on the yz-plane are exactly the G-polymers on that plane, for an appropriate choice of the graph G. Our plan for computing the total volume of the space of order-n polymers in $\mathbb{R}^3$ is to use Theorem 4 to compute the (lower-dimensional) volume of the space of polymers with given x-axis projection, then integrate over all possible x-axis projections. This seems more complicated than in the 2-dimensional case, but in fact gives us additional information.

Lemma 6. *The $(n-1)$-dimensional volume of the set of polymers whose centers project to $x_1 < \cdots < x_n$ is an integer multiple of $(2\pi)^{n-1}$ and depends only on the set of pairs i, j with $|x_j - x_i| \le 1$.*

Proof. In any such polymer, the distance between the yz-plane projections of each pair i, j of adjacent centers is determined by $|x_i - x_j|$; in fact the distance r_{ij} satisfies $(x_i - x_j)^2 + r_{ij}^2 = 1$. For nonadjacent centers, this distance is at least r_{ij} provided $|x_i - x_j| \le 1$; otherwise it is unconstrained.

It follows that if we let G be the graph on vertices $\{1, \ldots, n\}$ in which i is adjacent to j if and only if $|x_i - x_j| \le 1$, then by Theorem 4 the desired volume is $\mu(G)(2\pi)^{n-1}$, where $\mu(G) = |\mathcal{T}_G(1, 0)|$. ∎

Computing the volume. A *unit interval graph* (see, e.g., [**12**]) is defined by a set of unit-length intervals on the real line; it has one vertex for each interval and two intervals are adjacent in the graph just when they overlap. The graph G in the above proof is such a graph, with the intervals centered at the x_i.

The value $|\mathcal{T}_G(1, 0)|$ is easy to compute for unit interval graphs. Order the edges lexicographically according to their (ordered) endpoints; that is, edge $\{i, j\}$ (with $i < j$) precedes edge $\{i', j'\}$ (with $i' < j'$) if $i < i'$ or if $i = i'$ and $j < j'$. With this ordering, the safe spanning trees of G are those which are inductive in the sense of the introduction: all paths from the root 1 have increasing indices. It follows that each vertex $j > 1$ has as its parent some $i < j$ for which $x_j - x_i \le 1$. Thus,

$$\mu(G) = \prod_{j=2}^{n} \gamma(j) ,$$

where $\gamma(j)$ is the number of $i < j$ for which $x_j - x_i \le 1$.

It follows that the volume of the 3-dimensional polymer configuration space is

$$\begin{aligned} \mathrm{Vol}(\mathrm{BP}_{K_n}) &= (2\pi)^{n-1} \int_D n!\, \mu(G)\, dx_2 \cdots dx_n \\ &= (2\pi)^{n-1} \int_D n! \prod_{j=2}^{n} \gamma(j)\, dx_2 \cdots dx_n . \end{aligned} \tag{1}$$

Here the $n!$ factor appears because of the relabelling of the balls, D is the domain defined by $\{0 = x_1 \le x_2 \le \cdots \le x_n\}$ and G is the interval graph defined from $\{0 = x_1, x_2, \ldots, x_n\}$.

Let T_n be a uniformly random tree on the labels $\{1, \ldots, n\}$, with an independent uniformly random real length u_{ij} in $[0, 1]$ assigned to each edge $\{i, j\}$. Choose a root for T_n uniformly at random. For each $j = 1, \ldots, n$ let a_j be the sum of the lengths of

the edges in the path from the root to j in T; and let $0 = b_1 \le b_2 \le \cdots \le b_n$ be the a_i taken in order. Let $\mathbf{B}$ be the (random) vector $(b_1, \ldots, b_n)$.

Theorem 7. *The total volume of the configuration space of 3-dimensional branched polymers of order n is $n^{n-1}(2\pi)^{n-1}$. Moreover, if X be a random branched polymer, and $x_1 \le x_2 \le \cdots \le x_n$ the projections of its centers onto the x-axis, then, after translating so that $x_1 = 0$, the random vector $(x_1, x_2, x_3, \ldots, x_n)$ is distributed exactly as $\mathbf{B}$.*

Proof. Given the points $0 = x_1 < \cdots < x_n$, construct a labeled tree rooted at vertex 1 by attaching each vertex j to some $i < j$ satisfying $|x_i - x_j| \le 1$; there are $\prod_{j=2}^{n} \gamma(j)$ ways to do this. We can think of each such tree as having edge lengths given by the $|x_i - x_j|$.

If we then arbitrarily reassign labels $\{1, 2, \ldots, n\}$ to the vertices, we obtain $n! \prod_{j=2}^{n} \gamma(j)$ trees in all, each bearing the same relation to the $x_1, \ldots, x_n$ that the trees T_n considered above have to $b_1, \ldots, b_n$. We can evaluate the integral in (1) by computing the sum over these labeled trees of the integral over the set of $x_2, \ldots, x_n$ which can give rise to that tree. However, the set of $x_2, \ldots, x_n$ which can give rise to a given labeled tree has volume exactly 1, since each edge of the tree can have any length in [0, 1], independently of the others. Thus, each labeled tree contributes the same amount, 1, to the integral.

By Cayley's theorem (see, e.g., [**9**, Chapter 2]), the number of rooted labeled trees on n nodes is n^{n-1}. Thus $\mathrm{Vol}(\mathrm{BP}_{K_n}) = (2\pi)^{n-1} n^{n-1}$.

Since each tree contributes the same amount to the total volume, the second statement follows. ∎

Theorem 7 says that the x-axis projections of a random $X \in \mathrm{BP}_n$ can be obtained by planting the root of T_n at $x = 0$ and stretching the tree to the right, letting the rest of its nodes mark the projections. Figure 6 illustrates the case $n = 4$. The rows are indexed

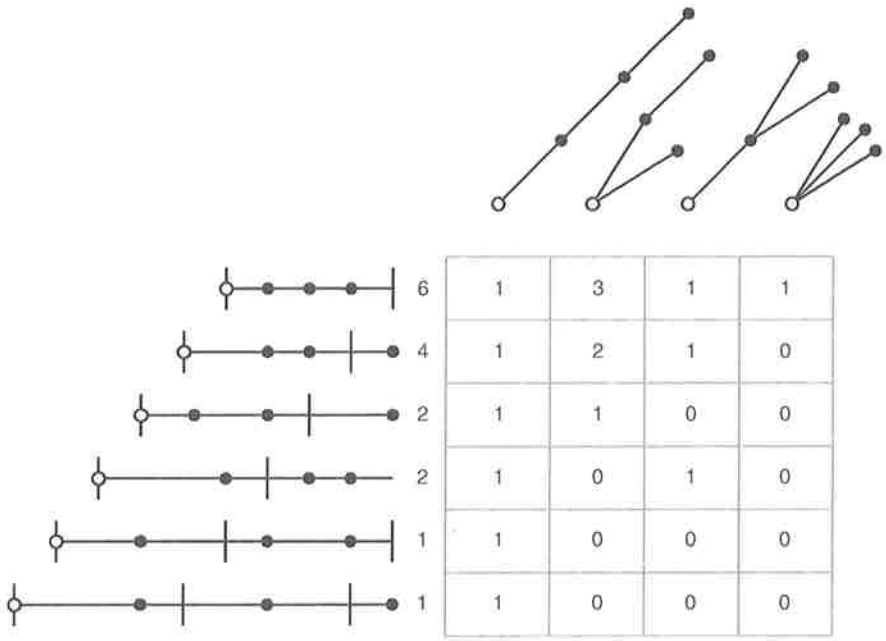

Figure 6. The matrix of interval graphs and (unlabeled) trees for $n = 4$.

by interval graph types G, presented as sample projections, each accompanied by its relative volume $\mu(G)$. The columns are indexed by trees, each weighted by the number of ways it can arise from an interval graph.

Note that the theorem does *not* say that the tree structure of a random 3-dimensional polymer is uniformly random; for example, no polymer can have a node of degree greater than 12.

From Theorem 7 we can incidentally deduce the nonobvious fact that the "reverse" vector $(0, b_n - b_{n-1}, b_n - b_{n-2}, \ldots, b_n)$ has the same distribution as $\mathbf{B}$.

Theorem 8. *The expected diameter (combinatorial or Euclidean) of a random 3-dimensional polymer grows as* $n^{1/2}$.

Proof. Szekeres' Theorem (see [**11, 16**]) says that the expected length of the longest path in a random tree on n labels is of order $\sqrt{n}$. The expected length of the longest path from the root in our edge-weighted tree T_n must therefore also be of order $\sqrt{n}$, and this is exactly the length of the projection of our random polymer on the x-axis. Since the space of polymers is independent of the choice of axes, the spatial diameter of a random polymer must also be of order $\sqrt{n}$. (If the diameter were significantly larger than the diameter of its projection to the x-axis, then almost all random rotations of the polymer would result in a longer x-axis diameter.) ■

5. PROOF OF THE INVARIANCE LEMMA. We now return to the Invariance Lemma, which states that the volume of the space of planar polymers of order n does not depend on their radii. As noted above, the proof works for the more general G-polymer case as well.

Recall that given a polymer $X = X(R)$, with radius vector R, the graph $H(X)$ has a vertex at the center of each disk and an edge between vertices whenever the corresponding disks are adjacent. When (as almost surely) $H(X)$ is a tree, we root $H(X)$ at the origin, and direct each edge away from the origin. Let $e_1, \ldots, e_{n-1}$ be the edges of $H(X)$ (chosen in some order) and $\theta_1, \ldots, \theta_{n-1}$ the corresponding "edge angles."

For a given combinatorial tree T (with labeled vertices), the set of polymers $X = X(R, T)$ with graph $H(X) = T$ can thus be identified with a subset of $[0, 2\pi)^{n-1}$. Call this set $\mathrm{BP}_R(T)$ (this is shorthand notation for $\mathrm{BP}_{K_n(R)}$). The boundary of $\mathrm{BP}_R(T)$ corresponds to polymers having at least one cycle; the corresponding plane graphs $H(X)$ are obtained by adding one or more edges to T. Indeed, the boundary of $\mathrm{BP}_R(T)$ is piecewise smooth and the pieces of codimension k correspond to polymers with k elementary cycles (i.e., k edges must be removed from H to make a tree).

A polymer X with cycles lies in the boundary of each $\mathrm{BP}_R(T)$ for which T is a spanning tree of the graph $H(X)$. Each such $\mathrm{BP}_R(T)$ will contribute its own parametrization to X. Note, however, that some trees may be unrealizable by unit disks (e.g., the star inside a 6-wheel); for such trees T, $\mathrm{BP}_R(T)$ has zero volume.

We can construct a model for the parameter space of all polymers of size n and disk radii R by taking a copy of $\mathrm{BP}_R(T)$ for each possible combinatorial type of tree, and identifying boundaries as above. Note that the identification maps are in general analytic maps on the angles: in a polygon with k vertices whose edges have fixed lengths $r_1, \ldots, r_k$, any two consecutive angles are determined analytically by the remaining $k - 2$ angles. This space is, however, difficult to understand on its own. Are there other coordinates in which it has a nice geometric structure?

Perturbations. Let P be a polygon with edges $1, 2, \ldots, m$, numbered and oriented counterclockwise. Assuming its edge lengths are fixed, P is determined up to translation by the edge angles $\phi_1, \ldots, \phi_m$ of its sides.

The space of perturbations of the m-gon P which preserve its edge lengths is $(m-2)$-dimensional, and is generated by "local" perturbations which move only two consecutive vertices and thus the three edges incident to them. Here by perturbation we mean the derivative at 0 of a smooth one-parameter path in the space of m-gons with the same edge lengths as P. Such a perturbation is determined by the derivatives of the angles ϕ_i with respect to the parameter t along the path. We define $\partial/\partial t_i$ to be the infinitesimal perturbation of P, preserving the edge lengths, for which $\partial\phi_j/\partial t_i = 0$ unless j is one of $i, i+1, i+2$ (indices chosen cyclically) and $\partial\phi_i/\partial t_i = 1$. See Figure 7. (If $\phi_{i+1} = \phi_{i+2}$, this perturbation is not well defined; we assume that P is in general position so this problem does not arise.)

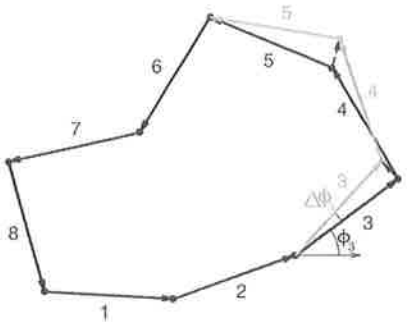

Figure 7. Local perturbation of edge 3 of an octagon.

The $\partial/\partial t_i$ for $i = 1, 2, \ldots, m-2$ generate all edge-length-preserving perturbations of P. These $\partial/\partial t_i$ are useful because they provide local infinitesimal coordinate charts for the boundaries of the various sets $\mathrm{BP}_R(T)$ which share the same m-cycle. Note that the rigid rotation of P is in the space generated by the $\partial/\partial t_i$.

Suppose that $\mathrm{BP}_R(T)$ for some T is parametrized by angles $\theta_1, \ldots, \theta_{n-1}$, and we are on a point of the boundary defined by an m-gon P with edge angles $\phi_1, \ldots, \phi_m$. Note that $m-1$ of the ϕ's, modulo π, occur among the $\theta_1, \ldots, \theta_{n-1}$. This boundary is locally an $(n-2)$-manifold M; but we will fix all angles not occurring in P, since they do not play a role in what follows, reducing M to an $(m-2)$-manifold. Nearby points on the boundary correspond to polymers with the same cycle, but realized by slightly perturbed m-gons with edge lengths preserved.

We also need to consider perturbations of P which change the edge lengths. Let $\partial/\partial S$ be a smooth perturbation of M which changes one of the radii, say r_1, infinitesimally. That is, S moves each polygon on M to a nearby polygon with perturbed edge lengths. Applying this perturbation will in particular move M off of itself.

Volumes

Conservation. Here we determine how the volume of $\mathrm{BP}_R(T)$ changes when one of the radii is increased. We begin by restating the Invariance Lemma:

Lemma 9. *The total volume of the space of branched polymers in $\mathbb{R}^2$, $B_R^2(n)$, does not depend on the radii R of the disks.*

Proof. We will prove the stronger fact that the *local* volume change under a small change in radii is zero. That is, near a polymer on the boundary of the configuration space, the volumes of the parts of the configuration space lost or gained under a small change in radii sum to zero.

As above let P be an m-gon in a polymer in the boundary of $\mathrm{BP}_R(T)$. We can assume that P is the only cycle: otherwise we would be on a codimension-2 part of the boundary which will not contribute to the total volume change. Let M be the $(m-2)$-manifold which is the part of the boundary of $\mathrm{BP}_R(T)$ near P when we have fixed the angles of all edges not in P. When we apply an infinitesimal perturbation to the radii which increases r_1, we can compute the change in the volume of $\mathrm{BP}_R(T)$ by integrating, along the boundary, the infinitesimal change at each point on the boundary. We need, then, only compute the local volume element under the perturbation $\frac{\partial}{\partial S}$. We will show that the sum of these local volume elements is zero.

Let A be an $m \times m$ square matrix whose first row is the all-ones vector, and for which $\det A = 0$. Let B be the $(m-1) \times m$ matrix obtained from A by removing the first row. Expanding $0 = \det A$ along the first row, we deduce that the alternating sum of the $(m-1) \times (m-1)$ minors of B is zero: letting v_j be the jth column vector of B, we have

$$\sum_{j=1}^{m} (-1)^j v_1 \wedge \cdots \wedge \widehat{v_j} \wedge \cdots \wedge v_m = 0, \tag{2}$$

where $\widehat{v_j}$ indicates that the entry v_j is missing from the jth term, and $v_1 \wedge \cdots \wedge \widehat{v_j} \wedge \cdots \wedge v_m$ denotes the determinant of the matrix whose columns are the v's.

In the above let $\phi_1, \ldots, \phi_m$ be the edge angles of the sides of P, and B the matrix whose ij-entry is $\partial\phi_j/\partial t_i$ for $i = 1, \ldots, m-2$ and whose last row is $\partial\phi_j/\partial S$ for $j = 1, \ldots, m$ (see equation (3) below). Since the rigid rotation of P is in the space generated by $\partial\phi_j/\partial t_i$, the all-ones vector is a linear combination of the first $m-2$ rows of B. In particular the matrix A obtained from adding a row of 1's to B has determinant 0, and so we have (2).

We can, however, interpret the jth summand in (2), when integrated over M (and over the edges not included in P) as (up to sign, at least) the infinitesimal change in volume of $\mathrm{BP}_R(T_j)$ under the perturbation S, where T_j runs over the trees obtained by removing one edge of P. Once we have seen that the signs work out correctly, then, by (2), the net infinitesimal volume change of $\mathrm{BP}_R(T_j)$, when summed over j, is zero.

Because of the factor $(-1)^j$ in (2), the signs work out correctly if and only if the vector $\partial/\partial t_1 \wedge \cdots \wedge \partial/\partial t_{m-2}$ (by this we mean the cross product of these $n-2$ vectors: the vector perpendicular to these and of length equal to their determinant on the subspace they span) considered as a normal vector to the boundary of $\mathrm{BP}_R(T_j)$, represents alternately the outward and inward normal to this boundary of $\mathrm{BP}_R(T_j)$ as j runs from 1 to m. In particular, we need to show that the orientation of this normal vector changes (from outward to inward or vice versa) when going from j to $j+1$. To check this, take the vector $\partial/\partial S_j$ which increases (only) the radius r_j of the ball between edges j and $j+1$. This vector has positive component in the outward normal directions for both $\mathrm{BP}_R(T_j)$ and $\mathrm{BP}_R(T_{j+1})$, since increasing the radius of the jth ball decreases the space available to T_j and T_{j+1}. However, $\partial\phi_i/\partial S_j$ is zero unless $i = j$ or $j+1$ and the nonzero components $\partial\phi_j/\partial S_j$ and $\partial\phi_{j+1}/\partial S_j$ have opposite sign. So the two $(m-1) \times (m-1)$ minors of

$$\begin{pmatrix} \frac{\partial \phi_1}{\partial t_1} & \cdots & \frac{\partial \phi_j}{\partial t_1} & \frac{\partial \phi_{j+1}}{\partial t_1} & \cdots & & \frac{\partial \phi_m}{\partial t_1} \\ \vdots & & & & & & \vdots \\ \frac{\partial \phi_1}{\partial t_{m-2}} & \cdots & \frac{\partial \phi_j}{\partial t_{m-2}} & \frac{\partial \phi_{j+1}}{\partial t_{m-2}} & \cdots & & \frac{\partial \phi_m}{\partial t_{m-2}} \\ 0 & \cdots & \frac{\partial \phi_j}{\partial S_j} & \frac{\partial \phi_{j+1}}{\partial S_j} & 0 & \cdots & 0 \end{pmatrix} \tag{3}$$

obtained by removing the jth or $(j+1)$st column have opposite sign. Therefore we need to put in the sign change in (2) in order to make both represent the actual changes in the volumes of $\mathrm{BP}_R(T_j)$ and $\mathrm{BP}_R(T_{j+1})$ under $\partial/\partial S_j$ (and therefore under any perturbation of the radii). ■

Explicit formulae. The relative volume changes for the different $\mathrm{BP}_R(T_i)$ as functions of the shape of P have a surprisingly simple formula.

Proposition 10. *Let P be an m-gon as above with edges $e_1, \ldots, e_m$ in counterclockwise order. The local volume change near P of $BP_R(T_i)$ due to an increase in radius r_1 (of the ball centered at the vertex between edges e_1 and e_2) is proportional to the dot product of e_i and the vector w in direction $\frac{1}{2}(\phi_1 + \phi_2)$, that is, perpendicular to the angle bisector.*

Note that since the vectors e_i sum to zero, so do their dot products with w. This gives a restatement of the invariance principle.

Proof. Let M_i be the ith $(m-1) \times (m-1)$ minor of B, that is, $M_i = v_1 \wedge \cdots \wedge \hat{v}_i \wedge \cdots \wedge v_m$. The vector $V = (M_1, -M_2, M_3, \ldots, (-1)^{m+1} M_m)$ is in the kernel of B (since, upon adding a generic first row to B and inverting the resulting $m \times m$ matrix, the first column of the result is proportional to the above vector V). Therefore V is perpendicular to the rows of B.

Write $e_j = a_j e^{i\phi_j}$ in polar coordinates. From $\sum e_j = 0$ we get $d\left(\sum e_j\right) = \sum_j a_j i e^{i\phi_j} d\phi_j = 0$, or $\sum_j e_j d\phi_j = 0$ for any perturbation of the closed polygon P fixing edge lengths. In particular the vector $(e_1, \ldots, e_m) \in \mathbb{C}^m$ is perpendicular to the first $m-2$ rows of B. Finally, let w be the vector $e^{i(\phi_1+\phi_2)/2}$ and denote by $\langle e_j, w \rangle$ the component of e_j in direction w. The vector $(\langle e_1, w \rangle, \langle e_2, w \rangle, \ldots, \langle e_m, w \rangle)$ is perpendicular not just to the first $m-2$ rows of B but also to the last row: the last row is zero in all but the entries 1 and 2, and the values there are explicitly $\frac{1}{a_1} \cot((\phi_1 - \phi_2)/2)$ and $\frac{1}{a_2} \cot((\phi_2 - \phi_1)/2)$ respectively.[1]

We therefore see that V is proportional to $(\langle e_1, w \rangle, \langle e_2, w \rangle, \ldots, \langle e_m, w \rangle)$ as claimed. ■

6. BUILDING RANDOM POLYMERS IN THE PLANE. We now show how to construct inductively a uniformly random branched polymer of order n in the plane.

We begin with a unit disk centered at the origin. Suppose we have constructed a polymer of size $n-1$, $n > 1$. We choose a uniformly random disk from among the $n-1$ we have so far, then choose a uniformly random boundary point on that disk and

[1] This can be seen by taking $\partial/\partial S$ of the identity $(a_1 + S)e^{i\phi_1} + (a_2 + S)e^{i\phi_2} = \textit{constant}$ and solving for $\partial\phi_1/\partial S, \partial\phi_2/\partial S$.

start growing a new disk tangent to that point. If a disk of radius 1 fits at that point, this will define a polymer of size n.

Otherwise there is a radius r with $0 < r < 1$ at which a cycle P forms with the new disk and some other disks present. At this point our polymer X is in the boundary of the space $\mathrm{BP}_R(T)$, where $R = \{1, 1, \ldots, 1, r\}$, and we need to choose some other tree T' for which X is in the boundary of $\mathrm{BP}_R(T')$, and which has the property that increasing r (and leaving the angles fixed) will not cause the disks to overlap. There will be at least one possible such T' because the volume of $\mathrm{BP}_R(T)$ near X is decreasing as r increases and so must be compensated by an increase in volume of some $\mathrm{BP}_R(T')$. We choose randomly among the $\mathrm{BP}_R(T')$ with increasing volume, with probability proportional to the infinitesimal change in the volumes of the $\mathrm{BP}_R(T')$'s as r increases. This ensures that the volume lost to $\mathrm{BP}_R(T)$ as r increases is distributed among the other $\mathrm{BP}_R(T')$ so as to maintain the uniform measure.

Figure 8 shows snapshots of the construction of a random polymer, in the process of growing its third and fourth disks; Figure 9 shows a polymer of order 500 generated by this method.

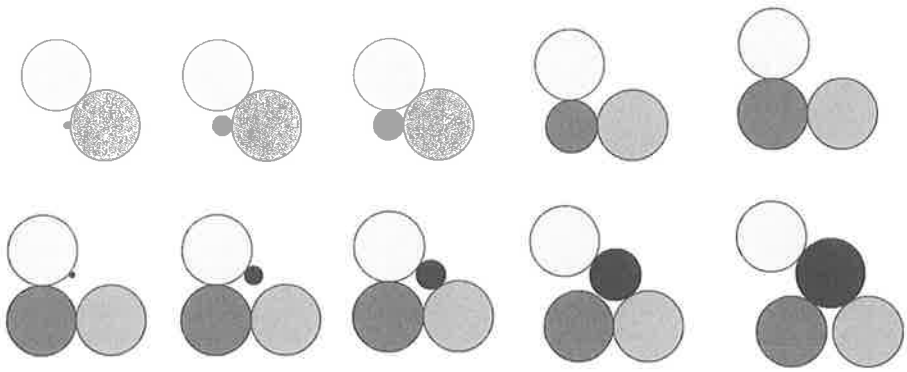

Figure 8. A random planar branched polymer growing new disks.

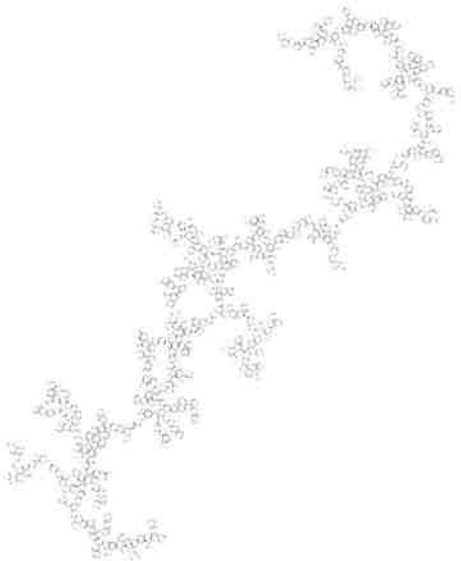

Figure 9. A uniformly random 2-dimensional branched polymer of 500 disks.

All of the above is easily generalized to produce uniformly random G-polymers for any connected graph G with specified edge lengths (and in fact we need this construction below, when generating 3-dimensional polymers). The vertices of G may be taken in any order $v_1, \ldots, v_n$ having the property that the subgraph G_k induced by $v_1, \ldots, v_k$ is connected for all k. When a uniformly random G_{k-1}-polymer has been constructed, a new point corresponding to vertex v_k is added coincident to a point uniformly chosen from its neighborhood—in other words, we start by assuming that the edges of G_k incident to v_k are infinitesimal in length. These edges are then grown to their specified sizes, breaking cycles when they are formed in accordance with the rules above.

7. CONSTRUCTING RANDOM POLYMERS IN 3-SPACE. To construct a uniformly random 3-dimensional branched polymer of order n, we first select a uniformly random labeled and rooted tree T from among the n^{n-1} possibilities. This can be done by means of a Prüfer code—see, e.g., [9]—which is itself just a sequence of $n-2$ numbers between 1 and n. The first entry of the code is the label of the vertex adjacent to the least-labeled leaf of T; that leaf is then deleted and succeeding entries defined similarly. The reverse process is also unique and easy. After T is constructed, its root k is chosen at random. In the constructed polymer, ball k will be the one whose center has least x-coordinate.

Edge-lengths are now chosen uniformly at random from $[0, 1]$ for the edges of T, and x_i is set to be the length of the path from vertex i to the root k of T. The numbers $x_1, \ldots, x_n$ will be the projections onto the x-axis of the ball centers, shifted so that the center of ball k projects onto the origin.

The unit-interval graph H is defined as above on the tree vertices, namely by connecting i to j if $|x_j - x_i| \leq 1$. Edge lengths are assigned to H by $\ell(i, j) = \sqrt{1 - (x_j - x_i)^2}$ so that the spheres of the polymer corresponding to tree vertices i and j are touching just when their centers lie at distance $\ell(i, j)$ when projected onto the yz-plane, and in any case lie at least that far apart. From the argument in the proof of Theorem 7 we know that given $x_1, \ldots, x_n$, the yz-plane projections are exactly a uniformly random planar H-polymer, which is then constructed using the methods of Section 6.

We now have the polymer's yz-plane projection, as well as its (shifted) x-coordinates; it remains only to translate the polymer along the x-axis so that the center of ball 1 lies at the origin.

Figures 10 and 11 are snapshots, from two angles, of a 3-dimensional branched polymer constructed as above.

8. OPEN PROBLEMS.

1. Is there a natural geometric structure on the space of polymers?
2. What are the volumes of $\mathrm{BP}_R(T)$ for each T when $R = (1, 1, \ldots, 1)$? Are they rational multiples of $(2\pi)^{n-1}$?
3. What is the expected diameter (combinatorial or geometric) of a random 2-dimensional branched polymer?
4. More generally, what do random polymers look like in the scaling limit, in any fixed dimension?

ACKNOWLEDGMENTS. This work began at a workshop of the Aspen Institute for Physics, and was motivated by a desire to understand the powerful results of David Brydges and John Imbrie [2]. The first author was supported by NSERC and by NSF grant DMS-0805493; the second, by NSF grant DMS-0600876.

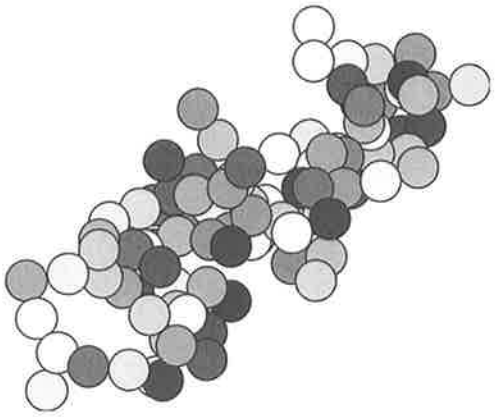

Figure 10. A random branched polymer in 3-space.

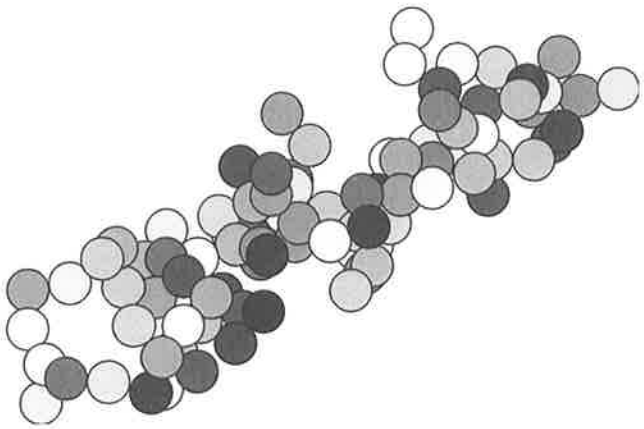

Figure 11. The same polymer, slightly rotated.

REFERENCES

1. N. L. Biggs, *Algebraic Graph Theory*, 2nd ed., Cambridge University Press, Cambridge, 1993.
2. D. C. Brydges and J. Z. Imbrie, Branched polymers and dimension reduction, *Ann. of Math.* **158** (2003) 1019–1039.
3. A. Bunde, S. Havlin, and M. Porto, Are branched polymers in the universality class of percolation? *Phys. Rev. Lett.* **74** (1995) 2714–2716.
4. H. H. Crapo, The Tutte polynomial, *Aequationes Math.* **3** (1969) 211–229.
5. F. Family, Real-space renormalisation group approach for linear and branched polymers, *J. Phys. A: Math. Gen.* **13** (1980) L325–L334.
6. L. A. Goldberg and M. Jerrum, Inapproximability of the Tutte polynomial, in *Proc. 39th ACM Symp. on the Theory of Computing 2007*, Association for Computing Machinery, New York, 2007, 459–468.
7. F. Jaeger, D. L. Vertigan, and D. J. A. Welsh, On the computational complexity of the Jones and Tutte polynomials, *Math. Proc. Cambridge Philos. Soc.* **108** (1990) 35–53.
8. D. J. Klein and W. A. Seitz, Self-similar self-avoiding structures: Models for polymers, *Proc. Natl. Acad. Sci. USA* **80** (May 1983) 3125–3128.
9. J. H. van Lint and R. M. Wilson, *A Course in Combinatorics*, Cambridge University Press, Cambridge, 1992.
10. L. S. Lucena, J. M. Araujo, D. M. Tavares, L. R. da Silva, and C. Tsallis, Ramified polymerization in dirty media: A new critical phenomenon, *Phys. Rev. Lett.* **72** (1994) 230–233.
11. A. Rényi and G. Szekeres, On the height of trees, *J. Aust. Math. Soc.* **7** (1967) 497–507.
12. F. S. Roberts, *Measurement Theory*, Addison-Wesley, Reading, MA, 1979.

13. D. Ruelle, Existence of a phase transition in a continuous classical system, *Phys. Rev. Lett.* **27** (1971) 1040–1041.
14. F. Spitzer, *Principles of Random Walk*, Van Nostrand, Princeton, NJ, 1964.
15. R. Stanley, *Enumerative Combinatorics*, vol. I, Wadsworth & Brooks/Cole, Monterey, CA, 1986.
16. G. Szekeres, Distribution of labeled trees by diameter, in *Combinatorial Mathematics X*, Lecture Notes in Mathematics, vol. 1036, Springer-Verlag, New York, 1982.
17. W. T. Tutte, *Graph Theory*, Addison-Wesley, Reading, MA, 1984.
18. C. Vanderzande, *Lattice Models of Polymers*, Cambridge Lecture Notes in Physics, No. 11, Cambridge University Press, Cambridge, 1998.
19. D. Vujić, Branched polymers on the two-dimensional square lattice with attractive surfaces, *J. Statist. Phys.* **95** (1999) 767–774.
20. G. N. Watson, *A Treatise on the Theory of Bessel Functions*, 2nd ed., Cambridge University Press, Cambridge, 1944.

RICHARD KENYON is Professor of Mathematics at Brown University. He held previous positions at the CNRS in Orsay, France and at the University of British Columbia. His interests include tilings, geometry, probability, and disc sports.
Mathematics Department, Brown University, Providence RI 02912, USA
richard.kenyon@brown.edu

PETER WINKLER is Professor of Mathematics and Computer Science, and Albert Bradley Third Century Professor in the Sciences, at Dartmouth. His research is mostly in discrete mathematics and the theory of computing; he has also written two books on mathematical puzzles, and in some circles is best known for his invention of cryptologic techniques for the game of bridge.
Department of Mathematics, Dartmouth College, Hanover NH 03755-3551, USA
peter.winkler@dartmouth.edu

Emily Dickinson and the Binomial Theorem

"I fancy you very often descending to the schoolroom with a plump Binomial Theorem struggling in your hand which you must dissect and exhibit to your incomprehending ones."

—Emily Dickinson, letter to her friend Susan Gilbert, Oct. 9, 1851.

At the time, Susan was teaching mathematics at Robert Archer's school for girls in Baltimore, MD. She married Emily's brother Austin in 1856. According to Susan's obituary, "as a young woman [she] was so good in mathematics that Prof. Hadley of Yale (the father of President Hadley), who for a time gave her instruction, told her that she ought to go to Yale college."

The quotation from Emily's letter can be found in T. H. Johnson, ed., *The Letters of Emily Dickinson*, Belknap Press, Cambridge, MA, 1958, p. 144. Susan Gilbert Dickinson's obituary is available at `http://www.emilydickinson.org/susan/obit.html`.